Reliability Engineering and System Safety 228 (2022) 108802

Contents lists available at ScienceDirect

Reliability Engineering and System Safety

journal homepage: www.elsevier.com/locate/ress

Critical damages identification in a multi-level damage stability assessment framework for passenger ships

Francesco Mauro [a,b,*], Dracos Vassalos [a], Donald Paterson [a]

[a] The Maritime Safety Research Centre, Department of Naval Architecture, Ocean and Marine Engineering (NAOME), University of Strathclyde, 100 Montrose St., G4 0LZ Glasgow, Scotland, UK

[b] Department of Maritime and Transport Technology, Faculty of Mechanical, Maritime and Materials Engineering, Delft University of Technology, Leegwaterstraat 17, 2628 CA Delft, the Netherlands

ARTICLE INFO

Keywords:
Ship safety
Flooding risk
Passenger ship
Damage stability
Collisions

ABSTRACT

The damaged stability assessment for a passenger ship is a process requiring the simulation of multiple damage scenarios. Nevertheless, the stochastic nature of the damage stability framework requires the analysis of a statistically significant number of cases. On the other hand, the probability density functions used to estimate the possible damage dimensions and locations along the ship generate many scenarios that are not critical for the ship's survivability, especially for large passenger ships. It is standard to apply empirical rules to restrict the number of damage scenarios, such as critical damages is only above two compartments, considering that damage stability regulations currently in force ensure survivability levels beyond this extent of breaches. However, a rigorous approach is lacking. To this end, in the present work, it is proposed to use more scientific-based methods to identify critical damages. This paper presents three original approaches developed in the context of a multi-level damage stability assessment. The first method relies on preliminary static calculations, the second on the energy absorbed by the ship during an impact, and the third on a purely dynamic approach. Here, the methods are critically compared on two sample passenger ships for collision damages, showing their respective advantages and disadvantages.

1. Introduction

Among the multiple hazards a passenger ship could face during its operational life, extensive flooding and consequent rapid capsize potentially lead to a higher number of fatalities. Therefore, an exhaustive analysis of risk associated with flooding events requires the development of pertinent risk models based on the information and parameters relevant and available during the different phases of the ship's life cycle [1]. Then, appropriate risk models should suit the design and operational phases, addressing diverse designers' and operators' needs. In the design phase, the information on the ship and operational profile entails a certain level of uncertainty, leading to a global probabilistic or deterministic safety measure, i.e. the Attained Survivability Index [2]. In the operational phase, the main ship parameters are fixed, allowing for a detailed study of specific operations and emergencies [3–5]. Recent literature on ship safety focuses mainly on the operational phase, considering the operational risk and its management [6–9], the waterway complexity and the risk mitigation [10–13] or a combination of the two aspects [4,5]. Works on the risk-based design marginally touch on the problem of flooding [14,15], focusing on other sources of risk like evacuation [16], fire [17], human factors [18,19] or collision avoidance [20].

Focusing on the design phase, the behaviour of a passenger ship in damaged conditions is one of the primary issues for marine safety [21]. Therefore, the survivability of passenger ships is a relevant attribute for the design of new vessels [22–24], influencing the consequent operational risk and mitigation measures [5]. However, the probabilistic calculation frameworks accepted and applied by designers for the attained survivability index assessment [25] employ static calculations [26] or simplified quasi-static methods [27], whilst more advanced and direct methodologies employing rigid-body time domain simulations are used mainly in the academy [28]. That is because, principally, passenger ship designers apply the damage stability studies outcome with a compliant-based approach and are threatened by the computational time required by complex flooding simulations. In fact, the probabilistic framework commonly used to quantify the final survivability requires evaluating about 10,000 breaches per damage type and drought [27,29]. The number of simulations becomes even

* Corresponding author.
E-mail addresses: F.Mauro@tudelft.nl (F. Mauro), d.vassalos@strath.ac.uk (D. Vassalos), donald.paterson@strath.ac.uk (D. Paterson).

https://doi.org/10.1016/j.ress.2022.108802
Received 27 April 2022; Received in revised form 21 July 2022; Accepted 3 September 2022
Available online 7 September 2022

Nomenclature

A	Attained survivability index
b	Auxiliary damage lateral penetration
B	Ship breadth
B_D	Potential damage lateral penetration
$B_{D_{max}}$	Maximum damage lateral penetration
E	Energy absorbed by the ship in the collision event
$_{i,j,k,h}$	Counters
I	Survival function for dynamic analyses
I_{side}	Damage side indicator
L_D	Potential damage length
L_s	Ship subdivision length
n	Number of damages composing a damage case
N_c	Number of damage cases
N_F	Number of filtered cases
N_r	Number of repetitions
N_s	Number of samples
N_u	Number of auxiliary uniform samples
p	Probability of occurrence of a specific damage or damage case
R	Required subdivision index
s	Probability to survive to a specific damage or damage case
T	Ship draught
t_{max}	Maximum simulation time
w	Weight between different damage types
X_D	Longitudinal position of potential damage centre
z_{LL}	Lower vertical limit of potential damage
z_{UP}	Upper vertical limit of potential damage
CFD	Computational Fluid Dynamics
DOF	Degrees of Freedom
EMSA	European Maritime Safety Agency
eSAFE	enhanced Stability After a Flooding Event
FLARE	Flooding Accident Response
ITTC	International Towing Tank Conference
MC	Monte Carlo
RANS	Reynolds Averaged Navier–Stokes
RQMC	Randomised Quasi-Monte Carlo
SOLAS	Safety of Life at Sea
TTC	Time to Capsize

more considerable while assessing survivability in adverse weather conditions because of the stochastic nature of irregular waves [28].

However, the probabilistic model of damage dimensions lead to many breaches not critical for vessel survivability, especially for large passenger ships [30]. Therefore, it is convenient to further analyse significant cases only with advanced dynamic analyses. A common but purely empirical approach to reducing this number is to consider only critical damage cases involving, for example, more than two adjacent zones. This approach could be valid from a design point of view but has no scientific basis. Other methods rely on the evaluation of static calculations without properly discussing the threshold adopted to filter out non-significant cases [31]. Therefore, there is a need for a rigorous approach to critical damage selection, to be used inside a damage stability framework capable to guide the designers in the transition between regulation-based safety calculations to more advanced direct flooding simulations and flooding risk assessment.

The present paper starts to fill this gap between the direct stability assessment tool potentially available to designers and the necessity to reduce the computational cases needed to assess passenger ship safety at the design stage. The process assesses three main targets, namely:

- Introduce a multi-level framework providing users with different grades of accuracy and calculation paths to assess stability.
- Adopt an advanced sampling technique reducing the uncertainties of the probabilistic assessment of flooding risk.
- Identify suitable damage filtering techniques to reduce the analyses to critical cases only.

All three objectives are in line with the main goal of the FLARE project, which is giving more importance to first principle-based tools for vessel survivability during the design process of a passenger ship [32]. The first point is covered by the presentation of a novel calculation framework that is flexible to use with different input sources and allows the user to select between static and dynamic calculations or a combination of the two. The framework adopts a novel sampling technique based on a Randomised Quasi-Monte Carlo (RQMC) method previously developed by the authors [33,34] and capable of reducing at least 2/5 of the initial number of breaches to be generated for the damage stability assessment, fulfilling the second point. And the third point is covered by the introduction of three alternative approaches to critical damage identification.

The three alternative explorative approaches aim at critical damages identification by employing non-empirical considerations. The procedures are here tested for the particular case of ship collisions, employing the probabilistic model for collision damages used in conventional damage stability assessment. The first method follows a traditional analysis of static survivability calculations, the second evaluates the critical scenarios based on the energy absorbed in the collisions, and the latter considers, for the first time in damage stability studies, dynamic simulations only.

The paper has the following structure. Section 2 describes the reference multi-level damage stability framework, focusing on the damage generation, the diverse levels of assessment, and the consequent need for damage filtering. Section 3 introduces the reference ships and the sample collision damages used in the study. Section 4 presents the static screening, Section 5 the energy method and Section 6 the novel approach based on dynamic simulations. The three filtering methods are then critically compared in Section 7, showing the advantages and disadvantages of the proposed solutions for critical damages identification.

2. Multi-level framework for damage stability assessment

The damage stability assessment of a passenger ship is a process that designers should tackle from the initial design stages. As a passenger ship is one of the most complex objects in engineering, the design process goes through various stages, constantly increasing the level of detail of internal layout and ship subsystems. Consequently, with damage stability being one of the highly relevant ship attributes, any change or advance in the project implies the reevaluation of the survivability, possibly increasing the detail and quality of the analyses.

For such a reason, the damage stability assessment should be flexible enough to cover different design phases, increasing the complexity of the calculations with the project progression. The conventional approaches to damage stability for passenger ships have different levels of approximations, significant outputs and computational effort [35–38]. However, it is customary for designers to treat this issue with a simplified regulation-compliant approach based on simplified calculations only [2,25]. Therefore, there is a need to provide a flexible framework capable of handling different levels of complexity for the

analyses, providing a clear workflow and combination of approaches for different design phases.

Firstly, there is the need to distinguish between the possible calculation approaches used to address damage stability. The following list gives an overview of the most commonly adopted methods to assess the survivability of a passenger ship, divided according to the motion equations resolutions and body forces calculations:

- ***Static calculations***:this is the most simplified analysis method based on hydrostatic calculations for the damaged condition. The results provide the residual GZ curve for the damaged ship for the final or intermediate stages of flooding;
- ***Quasi-Static simulations***: this analysis method evaluates the flooding progression with time, modelling the flooding rates according to Bernoulli's equation. However, the ship motions result from a static balance in 3-DOF (heave, roll and pitch) [39,40], eventually corrected by empirical coefficients for roll motion [41]. The water surface inside the compartments is assumed to be parallel to the undisturbed sea water level;
- ***Rigid-body dynamic simulations***: this method couples the simulation of water progression, based on Bernoulli's equation, together with the rigid body dynamics of the vessel in 4 to 6 DOF [42]. Such a method allows for predicting the behaviour of a damaged ship also in adverse weather conditions [28]. Various approaches differ for the modelling of the water motions inside the compartments. Assumptions start from simple quasi-static flat horizontal free-surface models [43,44]; the complexity arises with lumped mass [45] (that may consider also an inclined flat free-surface [46,47]) or dynamic resonance models [48] up to the adoption of the shallow-water equation [49,50];
- ***CFD simulations***: such techniques evaluate the internal motion of fluids from the numerical integration of RANS equations [51,52]. The methodology allows solving also the ship motion equations in 4 to 6 DOF, considering the fluid forces (both internal and external) as an external input to rigid body motion equations. This high fidelity method has a higher computational effort than the above-described methodologies.

A framework compliant with in-force regulations implies maintaining simplified methodologies for damage stability assessment. However, aiming for more physics-based damage stability results, a framework should include the possibility of using more advanced flooding simulations. In this respect, the adoption of high fidelity CFD calculations is not applicable due to the excessively high computational time needed for a single simulation. The necessity of performing numerous simulations to cover the possible damage cases while increasing results reliability suggests the adoption of time-domain simulations. Quasi-static codes satisfy computational time requirements; however, they are not advisable to simulate flooding progression in adverse weather conditions. Therefore, rigid-body dynamics simulations nowadays present the right balance between calculation accuracy and computational effort [21].

Fig. 1 outlines a multi-level framework that addresses the necessities of having both simple regulation-compliant calculations and advanced physics-based simulations. The process starts with the generation of the ship's internal geometry, reflecting the actual design status of the vessel layout during the project phases. The second step is to generate the damage scenarios through a probabilistic or a direct approach. Afterwards, two predictions levels are available; the first includes static analysis only, and the second considers dynamic simulations.

The following passages provide an overview of the main steps of the framework, focusing on probabilistic collision damages. This description allows for identifying the processes needed to detect potentially critical cases.

2.1. Damage breach generation

A framework for passenger ship survivability assessment after flooding necessitates the definition of breaches dimensions and locations for different kinds of damage types, e.g. collisions or groundings. Regardless of the damage type, there are two distinct methods for determining distributions of damage characteristics, depending on the desired level of accuracy and the availability of adequate tools and datasets, namely a probabilistic and a direct one.

The direct method derives damage characteristics distributions from scenario-based simulations implying the hindcast analysis of traffic routes in a given area [3,53] and the execution of crash analyses to determine the damage dimensions [54]. Such an approach uses first principle based-tools. Thus, it potentially provides a more realistic estimation of the damage dimensions, specific for the structural layout of the analysed ship. Therefore, the damage distributions are not general and require an update for any structural design change in the project. On the contrary, the probabilistic method provides a set of distributions independent of the internal and structural layout. Initially, the procedure was suitable for collision damages only, implemented in a zonal approach [55,56] as prescribed in SOLAS2009 [25]. Further developments in projects EMSA [57,58] and eSAFE [26,59] extended the probabilistic method to other relevant hazards for passenger ships, such as side and bottom groundings.

At the same time, the generation of breaches follows a direct non-zonal approach, where damage size and location are generated from marginal distributions by a Monte Carlo (MC) sampling method [58]. The MC sampling is subject to uncertainties. Therefore, at least 50,000 damage breach samples ensure convergence with the adopted damage breach distribution for assessing the vessel survivability for one loading condition. A recent development within FLARE project proposes the adoption of a Randomised Quasi-Monte Carlo (RQMC) sampling allowing a significant reduction of cases due to the lower variance of the sampling process [34]. A brief description of MC and RQMC sampling methods is provided in Appendix A.

This study focuses on collision damages, usually named C00 damages, in the probabilistic damage stability framework. The non-zonal definition of C00 damage follows the SOLAS zonal background [25], thus introducing the lower vertical limit of the breach [26]. Therefore, the geometrical model of a non-zonal C00 model requires the description of the following characteristics:

- longitudinal position of the potential damage centre X_D (m);
- longitudinal extent of the potential damage L_D (m);
- lateral penetration of the potential damage B_D (m);
- lower vertical limit of the potential damage z_{LL} (m);
- upper vertical limit of the potential damage z_{UL} (m);
- flag distinguishing starboard ($I_{side} = 1$) and portside ($I_{side} = -1$) damages.

Fig. 2 gives an overview of the geometrical model of C00 collision damages and the independent marginal cumulative distributions of the mentioned breach characteristics in non-dimensional form. Starboard and portside damages are equiprobable, while Appendix B reports the probabilistic description of the characteristics of C00 collision damages. The damage is defined as potential, meaning that it could also extend outside the vessel limits. This aspect requires particular attention for the positioning of the damage at the ship extremities. In case the potential damage is fully contained within the ship length L_s, X_D corresponds to the damage centre. If the damage partially extends outside the vessel, then the location of X_D should be changed as described in [60].

Even though marginal distributions are supposed to be independent, the potential damage penetration B_D and damage length L_D present an exception. The SOLAS framework implicitly assumes that for C00 damages, the ratio between dimensionless length and dimensionless

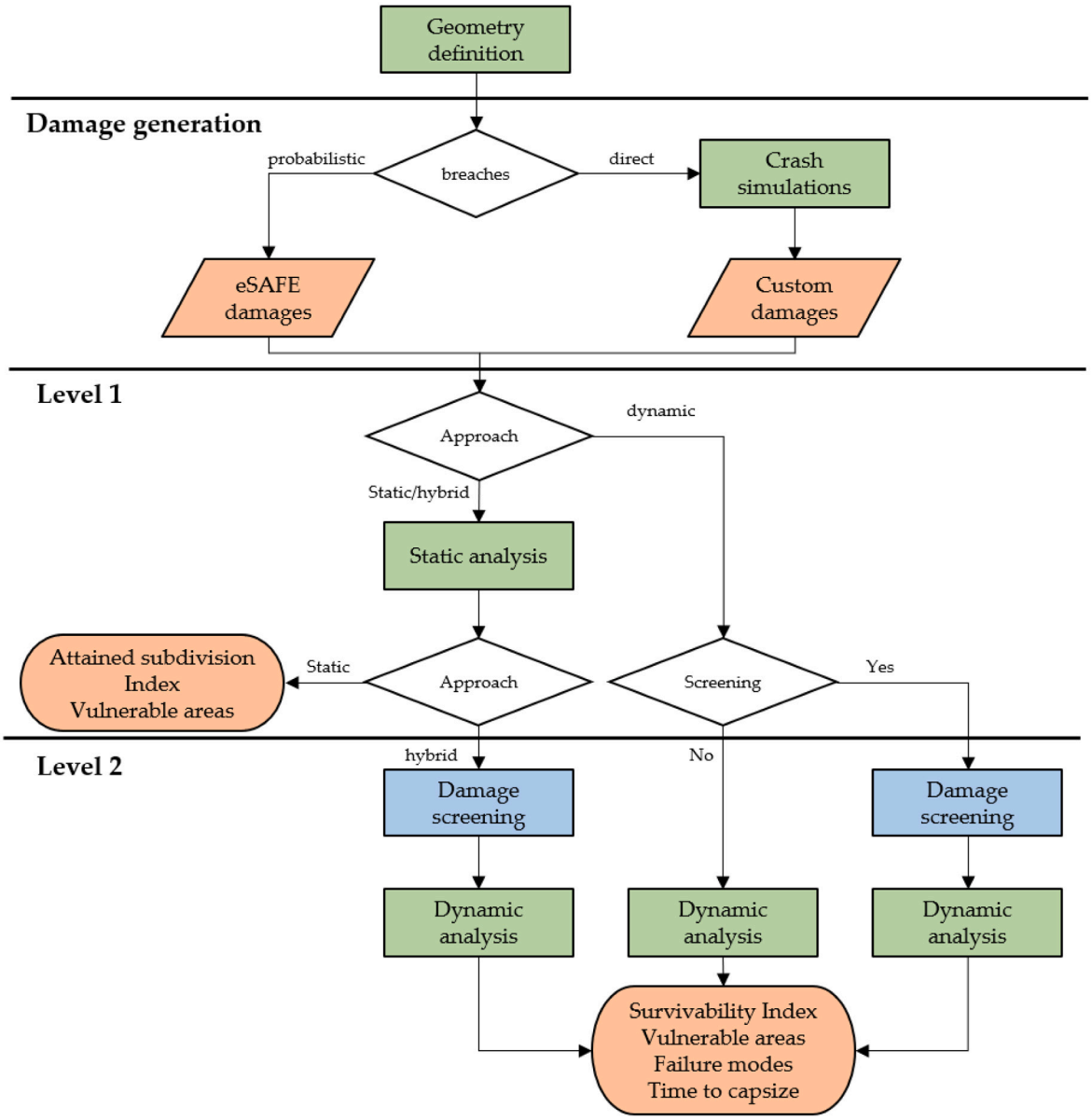

Fig. 1. Multi-level damage stability framework.

penetration cannot exceed 15. For such variables, an empirical rule avoids the generation of damages having too high relative penetration according to the following criteria:

$$B_{D_{max}} = \begin{cases} 15b\dfrac{L_D}{L_s} & \text{if } \dfrac{L_s}{L_D} < 30 \\ \dfrac{b}{2} & \text{if } \dfrac{L_s}{L_D} \geq 30 \end{cases} \tag{1}$$

where b is the local breadth of the ship at the considered waterline and L_s is the subdivision length. This truncation embedded in SOLAS can be handled with equivalent approaches for the direct generation of damages. The following algorithm provides a possible sequence for the generation of non-zonal collision damages:

1. Generation of I_{side}.
2. Generation of L_D.
3. Generation of X_D, checking the placement at the extremities according to L_D.
4. Sample an auxiliary b vector for damage penetrations.
5. Evaluate $B_{D_{max}}$ according to Eq. (1).
6. Obtain the final B_D distribution as $B_D = \min\left(b, B_{D_{max}}\right)$.
7. Generate z_{LL}.
8. Generate z_{UL}.

The non-zonal generation for collisions requires a multivariate sample on a six-dimension hypercube. Fig. 3 presents a set of 10^3 breaches sampled by the RQMC method considering the marginal distributions and the nomenclature presented in Fig. 2 for a $L_s = 198.0$ metres ship, thus neglecting for brevity the representation of I_{side}. This explanatory example uses a relatively low sample size to facilitate the graphical reproduction of the breaches population. However, the provided example is sufficient to show the capability of the RQMC method of evenly covering the design space and accurately reproducing the marginal distributions even with a low sample size. The graphs on the main diagonal represents the sampled dimensions of the breach in histogram form, compared with the associated marginal probability density function (reported in Appendix B). The off-diagonal graphs show the pairwise joint distributions of the random variables defining the breach dimensions in scatter form. As the random variables describing the damages are independent, the scatter plots are representative of

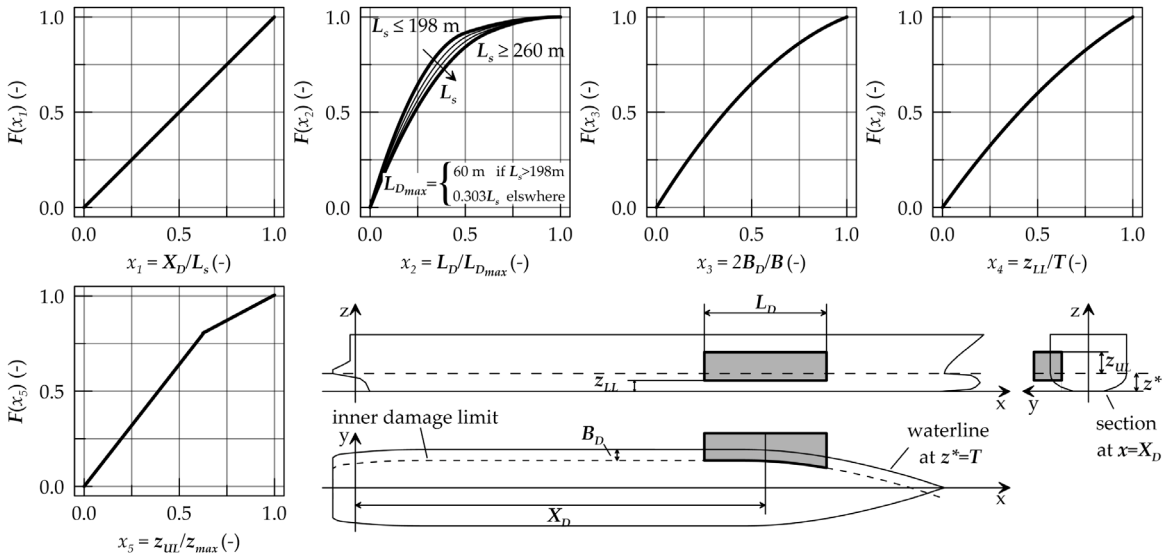

Fig. 2. Collision damages description and cumulative density functions.

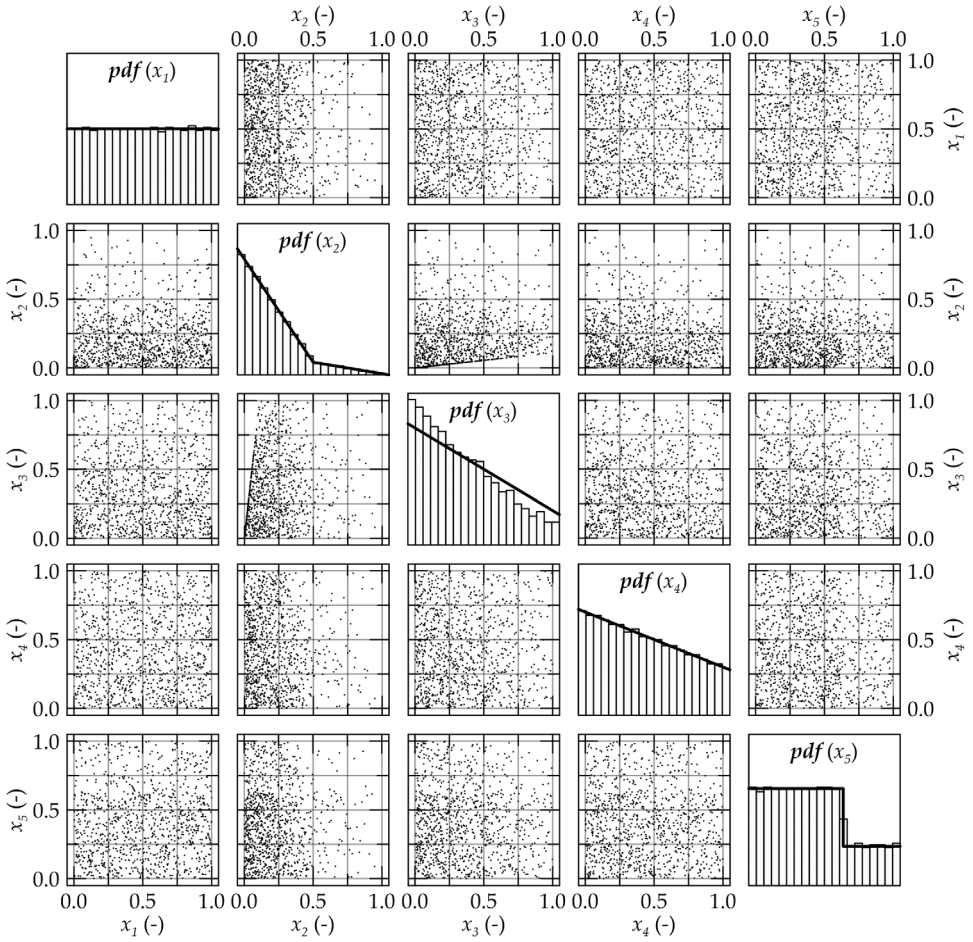

Fig. 3. Collision damages description and cumulative density functions.

uncorrelated values and the regions with more or less density of points derive from the associated marginal distributions. This is not true only for the joint distributions of L_D and B_D (x_2 and x_3, respectively).

A perusal of Fig. 3 allows detecting the effect of the empirical modification of damage penetration B_D according to Eq. (1). The sample probability density function of x_3 (described by the central histogram in Fig. 3) does not follow the original marginal distribution. The upper limit $B_{D_{max}}$ changes the steepness of the sample probability density function compared to the original marginal one, producing a final population with a higher density in the low penetration values. As a consequence, the joint scatter distribution between x_2 and x_3 presents a left bound (equivalent to the lower bound in the $x_3 - x_2$

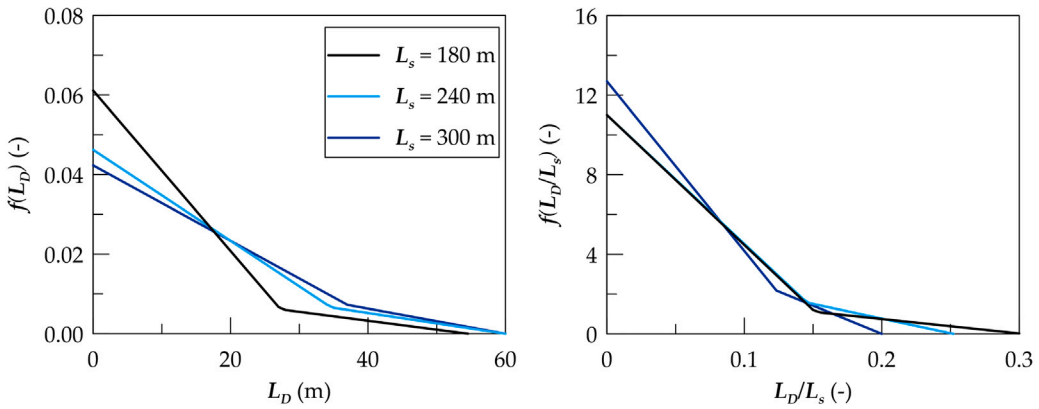

Fig. 4. Collision damages description and cumulative density functions.

joint distribution) corresponding to the associated $B_{D_{max}}$ value derived by Eq. (1). This effect intrinsically decreases the occurrence of damages with high penetration but does not directly decrease the potential vulnerability of the ship. As a last remark, the internal limit of the damage follows the waterline at $z^* = T$ shifted by B_D. Consequently, a C00 damage is not always box-shaped.

While generating C00 damages, attention should be paid to the L_D generation, as the distribution depends on the vessel subdivision length L_s. Fig. 4 presents an example of the different L_D distributions obtained by incrementally changing L_s. The maximum L_D limit of 60 metres for vessels above L_s=198 metres leads to distinct density functions for the higher L_D, resulting in a fatter tail than shorter ships. However, the higher damage length for long ships has a significantly lower ratio than the shorter ones, generating potentially less critical damages.

2.2. Level 1 assessment

The first level for damage stability assessment relates to static calculations. The process reflects the calculation techniques amended by SOLAS regulations [2] but applies the non-zonal approach with enhanced RQMC sampling [61]. The main target of the Level 1 assessment is the determination of ship survivability and the identification of possible vulnerable areas along the vessel. This assessment in the non-zonal framework is comprehensive of collisions, side and bottom groundings. Furthermore, a static analysis requires an additional step between damage sampling and survivability calculations. The non-zonal approach generates Ns breaches through the sampling process; however, several damages hit the same compartments in the ship. As a static analysis is not sensitive to the variation of the breach dimensions within a group of damaged rooms, such breaches identify a single damage case with a given occurrence.

The Attained subdivision index A gives the measure for survivability and is defined as follows by the in-force regulatory framework:

$$A = \sum_{k=1}^{3} \sum_{j=1}^{3} w_{jk} A_{jk} \tag{2}$$

where k indicates the damage type ($k = 1$ for collisions, $k = 2$ for bottom groundings and $k = 3$ for side groundings), j indicates the calculation draught (light service, partial or deepest subdivision droughts), w_{jk} are the weights between the calculation conditions, and A_{jk} are the partial indices evaluated on specific combinations of damage types and draughts. The partial A_{jk} of Eq. (2) have the following formulation:

$$A_{jk} = \sum_{i=1}^{N_c} p_{ijk} s_{ijk} \tag{3}$$

where i distinguishes each of the N_c groups of compartments that identify a unique damage case. The so-called p-factors p_{ijk} are associated with the occurrence of the specific damage case. Traditional methods derive p-factors from analytical integration for collision damages only [56], but adopting the non-zonal approach can be estimated by:

$$p_{ijk} = \frac{n_{ijk}}{N_s} \tag{4}$$

where n_{ijk} is the number of damages referring to the same damage case i, and N_s is the sample size. The s-factors s_{ijk} are linked to the probability to survive any specified damage. Their assessment through static calculations follows empirical formulations derived from the static residual GZ curve for all the intermediate and final stages of flooding associated with a damage case. The final attained subdivision index A is then obtained as a RQMC integration, to be compared with a regulatory required subdivision index R.

Furthermore, the p and s-factors are in a way key performance indicators of flooding risk. $p_{ijk}(1 - s_{ijk})$ gives a rough indication of the capsize probability associated with a particular damage case. Reporting $p_{ijk}(1 - s_{ijk})$ against the non-dimensional location of the damage centre X_D/L_s highlights the higher risk areas of capsizing due to flooding, thus where designers should focus on ship safety improvement. The static "risk" profile gives useful information to compare the vulnerability of different ships or design solutions.

Therefore, a Level 1 damage stability assessment provides designers with a regulatory compliant index determined by static calculations. Besides, the analysis identifies vulnerable areas to collision and groundings damage types. The same process can be used also considering custom damage distributions, but the Level 1 output offers no added significance for Class approval.

2.3. Level 2 assessments

Level 1 assessment is a simplified approach dealing with still water cases only, whilst allowing indirectly for impact of sea states through a wave height dependent s-factor [62]. However, detailed knowledge of the possible risk of capsizing due to flooding needs to consider a direct evaluation of the flooding process, including adverse sea conditions. Time-domain simulations based on rigid body dynamics are a good solution for dynamic modelling of a damaged ship in a seaway.

As earlier mentioned, time-domain simulations model the water ingress-egress from the breach. Therefore, breach dimensions influence the flow rate entering/leaving the ship, and breaches referring to the same damaged compartments lead to a different flooding process. For such a reason, the p-factors determination for each individual breach in static analyses is not necessary. Consequently, the partial survivability index given in Eq. (3) becomes as follows for dynamic analyses on N_s breaches:

$$A_{jk} = \frac{1}{N_s} \sum_{i=1}^{N_s} s_{ijk} \tag{5}$$

Therefore, Level 2 assessment requires a modification of the sampling process. In addition to the damage location and dimension, the RQMC process should determine the significant wave height H_s of the sea state of interest from a dedicated marginal distribution [63]. Such H_s is used to model an irregular sea state through a wave spectrum, generally utilising a Pierson–Moskowitz [64] for open seas or a JONSWAP [65] spectrum for limited fetch areas.

The spectral formulation fixes the wave amplitudes in the time-domain simulations, but phases are stochastic. Therefore only multiple repetitions N_r of the same sea state capture the nature of an irregular waves environment. Consequently, the survivability factor is the average of the N_r realisations of the same damage:

$$s_{ijk}|_{t_{max}} = \frac{1}{N_r}\sum_{h=1}^{N_r} I_h \tag{6}$$

The function I_h is equal to 1 if the vessel survives and 0 in case of capsizes within the maximum simulation time t_{max}. The simulation time strongly influences the survivability in a Level 2 assessment, especially for the simulation of irregular waves. The usual value for passenger ship survivability assessment is 30 min, but survival after 30 min does not necessarily imply that the considered scenario is safe. However, half an hour simulations are sufficient to identify the most critical scenarios for vessel survivability, namely transient capsize. Level 2 simulations are indeed appropriate to determine the nature of the capsize, which can be in the following flooding stages:

1. *Transient state*: the vessel capsizes in a time shorter or comparable with the natural roll period.
2. *Progressive state*: the ship survives the first transient phase but capsizes while the internal flooding process is still ongoing.
3. *Stationary state*: the vessel capsizes when there is no more significant water ingress or egress.

The transient capsize mode is the most impacting case for the loss of lives, as the capsize is too fast to start an evacuation process. However, not only transient events are critical for evacuations. According to the currently in force regulations for safety of passenger ships [66], the implicit minimum time criterion for the orderly vessel abandonment, which starts with the initiating flooding event and lasts until all persons have abandoned the ship, is the 3 h survivability. Therefore, the estimation of the time to capsize (TTC) is a crucial parameter for ship safety and, nowadays, is a primary design attribute for a passenger ship. The framework does not consider simulation higher than 30 min, but the estimation of the TTC distribution, also in a shorter time, can be an alternative key performance indicator of safety. In any case, the outcome of the Level 2 assessment in irregular waves has to be interpreted as an aleatory variable, both considering A index or TTC, being the final average value of multiple repetitions.

A Level 2 prediction can be pursued as a unique separate analysis, leading to a fully dynamic assessment of the vessel survivability or in addition to a static analysis. In the latter, the prediction can relate to a restricted set of damages only, leading to a hybrid approach. However, optimising the number of cases for Level 2 assessment necessitates a proper filtering strategy for damages.

2.4. Damage screening strategies

The framework described in Fig. 1 provides two different levels of accuracy for damage stability assessment. At the same time, several options are allowed concerning damage input and process. The damage stability assessment can stop with a Level 1 calculation, consider only a Level 2 calculation or combine the two levels. However, to limit the amount of Level 2 calculations, there is the need to implement reliable auxiliary processes to filter the cases to be analysed.

As highlighted in the framework description, a Level 2 assessment can be pursued as a standalone process (purely dynamic) or be complementary to Level 1 (hybrid). The two procedures have different necessities as, for the hybrid process, the filtering of critical cases can use static results. The pure dynamic process has not such information; therefore, it needs a different filtering strategy. The present study describes three methods conceptualised and developed for these two different scopes, namely:

- *Static results screening*: Level 1 static calculations results determine the critical cases using criteria related to the risk metric $p(1-s)$. This method is suitable only for the hybrid process.
- *Energy method*: this procedure evaluates the critical damages based on a simplified way to calculate the energy absorbed during the collision. This screening methodology is suitable for both hybrid and fully dynamic assessments.
- *Dynamic screening*: the process applies only to a fully dynamic assessment. A preliminary set of dynamic calculations in calm water determine the vulnerable areas to set up irregular waves simulations.

The following sections describe in detail the aforementioned filtering methods, showing a practical application example on two passenger ships.

Table 1
Ship-A and *Ship-B* main particulars.

Parameter	*Ship-A*	*Ship-B*	Unit
Length overall	162.00	300.00	m
Length between perpendiculars	146.72	270.00	m
Breadth	28.00	35.20	m
Subdivision draught	6.30	8.20	m
Height at main deck	9.20	11.00	m
Metacentric height	3.40	3.50	m
Displacement at subdivision draught	17267.40	50932.76	t
Deadweight	3800	8500	t
Gross tonnage	28,500	95,900	t
Number of passengers	1900	2750	–
Crew members	100	1000	–

3. Reference ships

The present study on critical damage detection and screening is using two reference passenger ships. For convenience, this section reports the two vessels' descriptions before using them as a worked example for the developed filtering procedures. As mentioned in the introduction, the reference vessels are a Ro-Pax vessel and a large cruise vessel, these being the selected test ships for most of the developments within the FLARE project. In this work, the Ro-pax will be named *Ship-A*, and the cruise ship, *Ship-B*. Table 1 gives the main parameters of the two vessels, and an overview of the general arrangements is in Fig. 5. *Ship-A* is representative of a medium to large passenger ferry, whilst *Ship-B* is a large cruise vessel. The ship sizes cover the two extremes in the range of breach length definition typical of collision damages described in the previous section, with *Ship-B* above 260 metres, and *Ship-A* below 198 metres. The general arrangement of the two ships reflects the granularity of the compartmentation used for the calculations, which is the definition level required for dynamic simulations.

3.1. Initial set of collision damages

The critical damage cases identification for the previously described damage stability framework requires sampling an initial set of breaches from pertinent probabilistic distributions for location and dimensions. With this specific study focusing on collisions, the damage characteristics derive from C00 damage type distributions. The most suitable and flexible method to generate damages in a damage stability framework follows a non-zonal approach.

Here, adopting an enhanced version of the process reduces sampling variance and, consequently, the number of samples. The sampling

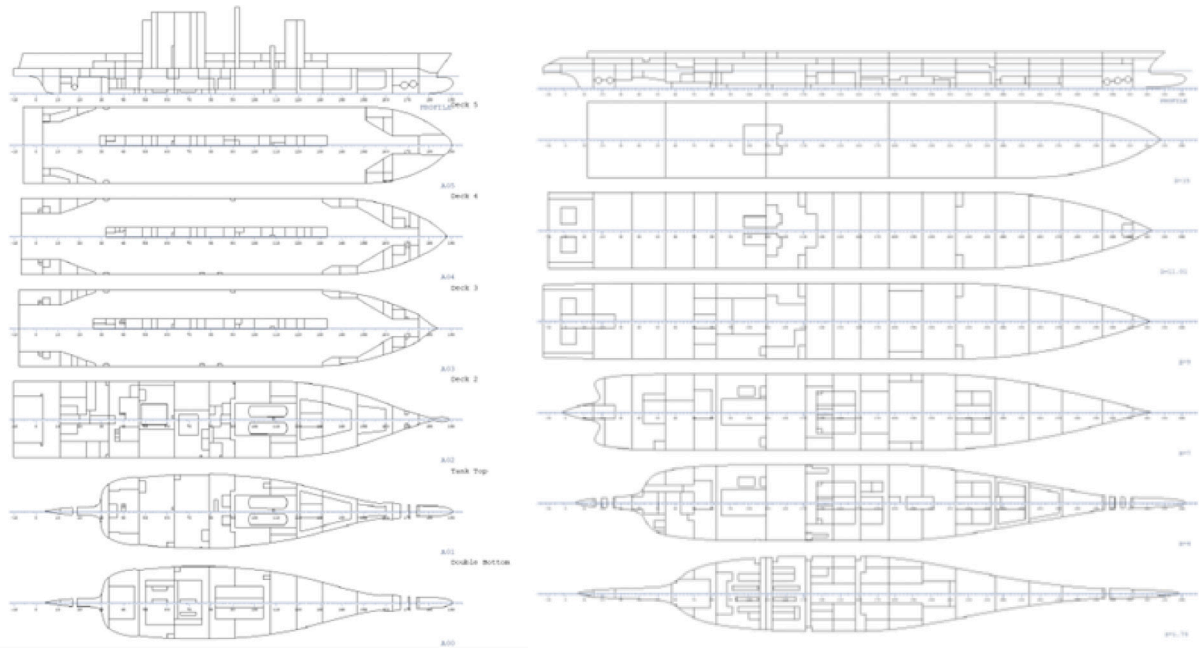

Fig. 5. Ship-A (*left*) and Ship-B (*right*) general arrangement.

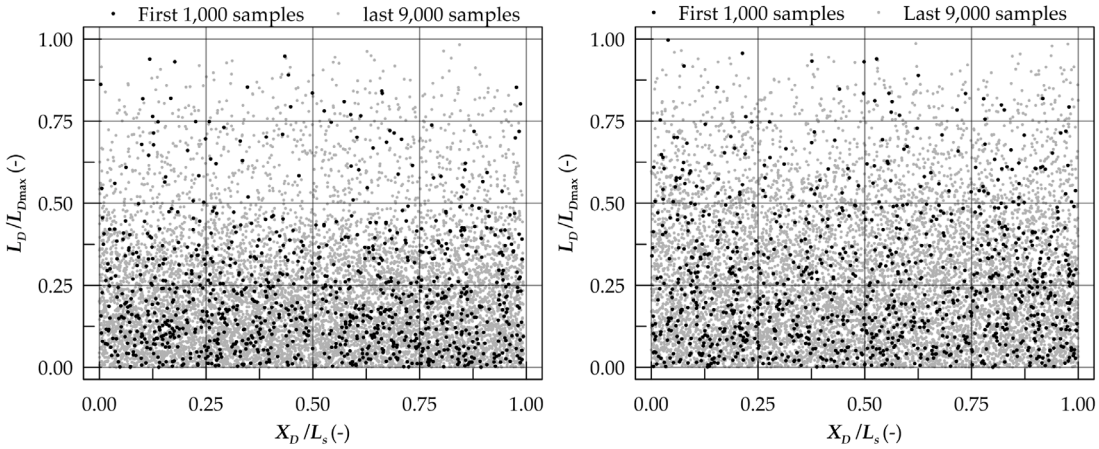

Fig. 6. Damage length sampling for Ship-A (*left*) and Ship-B (*right*).

process used to determine the damage cases is a RQMC process based on Sobol sequences, ensuring a more uniform coverage of the potential damage space than conventional pseudo-random methods. According to the indications provided in previous studies [33,34], the adopted damage set is composed of three samples repetitions of 10,000 breaches each.

In Fig. 6, the outcome of the damage sample is shown for *Ship-A* and *Ship-B*, respectively. The representation is limited to the distribution of damage length L_D at the respective longitudinal X_D position in non-dimensional form. The figure represents one of the three samples, highlighting the distribution of the first 1,000 samples compared to the total of 10,000 breaches. The different nature of the marginal distributions for damage length between the two ships (see Fig. 4) implies that, for *Ship-B*, there is a smoother transition between relatively short and long damages, whilst, for *Ship-A*, the density of relatively short damages is higher than for long ones. The differences in damage length distribution certainly affect the survivability of the two ships, including the detection of critical cases.

Both static and dynamic calculations for the two reference ships have been performed by employing PROTEUS3 software, which is based on the resolution of 4DOF rigid-body ship motion equations (surge and yaw are not considered), coupled with the floodwater dynamics. The flooding process is governed by the Bernoulli's equation, while the water inside compartments is modelled as a lumped mass. Froude–Krylov and restoring forces are integrated up to the instantaneous wave elevation both for regular and irregular waves. Radiation and diffraction are derived from 2D strip theory. Hydrodynamic coefficients vary with the attitude of the ship during the flooding process (heave, heel and trim). The vessel is assumed free to drift, with drift forces evaluated by empirical formulations. The simulations considers only the damaged (struck) ship, without considering the presence of the striking ship as usual in damage stability calculations. Further detailed information are given in [42].

4. Static results screening

A straightforward way to identify critical scenarios to be further analysed through dynamic simulations could derive from the analysis of static calculations. The static survivability assessment evaluates the damage cases derived from the sampling of marginal distributions, grouped in unique damage scenarios with associated p factors. Calculations performed on these cases allow determining the ship survivability

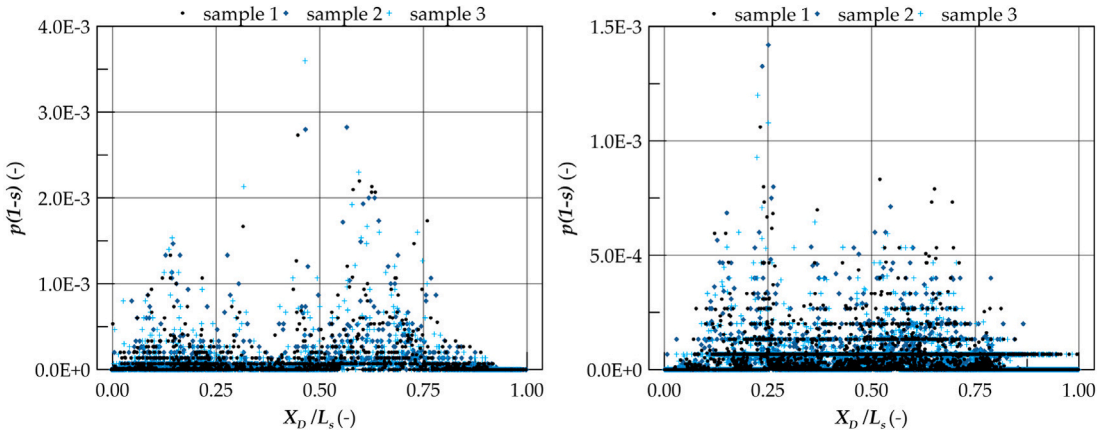

Fig. 7. Risk profile for Ship-A (*left*) and Ship-B (*right*).

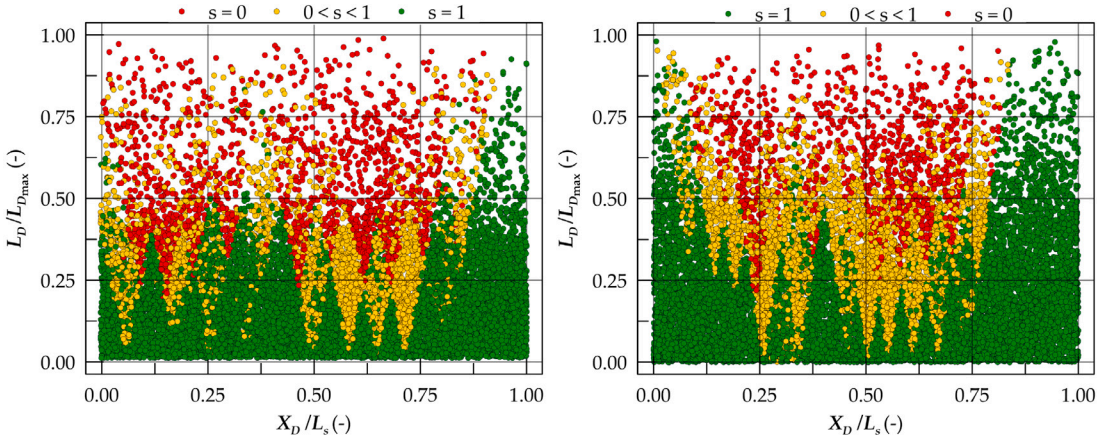

Fig. 8. s-factor for Ship-A (*left*) and Ship-B (*right*) considering all the sampled breaches.

for the associated damage scenario and evaluating the s-factor. From this analysis, the s-factor values are grouped into three categories:

- $s = 0$: cases where the vessel can be considered statically capsized or with insufficient residual stability margin.
- $0 < s < 1$: cases where there could be a reduced reserve of stability that may lead to capsizing in an irregular wave environment.
- $s = 1$: cases where the vessel can be considered safe and potentially has a sufficient reserve of stability to face waves.

Even though, as a first approximation, it can be considered that cases with s=0 lead to a dynamic capsize [31], it is wiser to consider the first two categories as those potentially leading to a capsize for dynamic simulations. The geometrical model used for static calculations includes fewer openings and compartments than the dynamic one. Therefore, a direct comparison is not possible between the two approaches. Usually, a static prediction is more conservative than a fully dynamic vulnerability assessment in calm water [22]. However, it is advisable not to discard a-priori all the undetermined cases, especially for irregular waves simulations.

As mentioned in the previous sections, the static calculations do not involve all the damage cases generated from the sampling procedures. The damage regrouping process reduces the number of cases where the s-factor needs to be evaluated, taking into account the weight of each single damage case through the p-factor. Consequently, the factor $p(1 - s)$ gives a rough estimate of the survival probability associated with a particular damage case.

In Fig. 7, an example is reported for the two passenger ships, highlighting the most dangerous areas of the two vessels, considering all three damage samples. The static calculations refer to the conditions reported in Table 1. Comparing the results in Fig. 7 for the two ships, it is noteworthy that *Ship-A* has an overall "risk" level higher than *Ship-B*. The latter can be further visualised in Fig. 8, representing the s-factor of every single damage of one sample as a function of non-dimensional damage position and length, thus neglecting the grouping present in the risk profile. Each point in the diagrams represents a potential case for further analyses with more advanced dynamic simulations. It is then straightforward to filter out all the damages with $s = 1$ (the green dots) and keep only the other cases for further analysis. Such a method filters out 66.5% of cases for *Ship-A* and 65.0% for *Ship-B*. Instead, considering only the points with $s = 0$, 88.9% and 91.7% of the damages can be filtered out for *Ship-A* and *Ship-B*, respectively.

It is also possible to mitigate the pure filtering based on the s factor, using the "risk" profile reported in Fig. 7. The damage cases reported in that figure are representative of the unique damage cases for static calculation. Thus, the damages with higher risk are those with $s \neq 0$ and a high p-value, which means damages that are more probable to face according to the reference probabilistic framework. Therefore, it can also be possible to consider as a filtering option the combined effect of both p and s, thus, a more appropriate risk metric. This procedure filters out all the damages under a given "risk" threshold. In Fig. 9, an example is given for the two ships, considering as "risk" threshold the value of 10^{-4}, which means considering only cases with $s = 0$ and intermediate unique damage cases having a global "risk" comparable to or higher than an immediate capsize. Therefore, this filtering reduces the damage cases where $0 < s < 1$, resulting in a number of filtered damages in-between the previously described simple options.

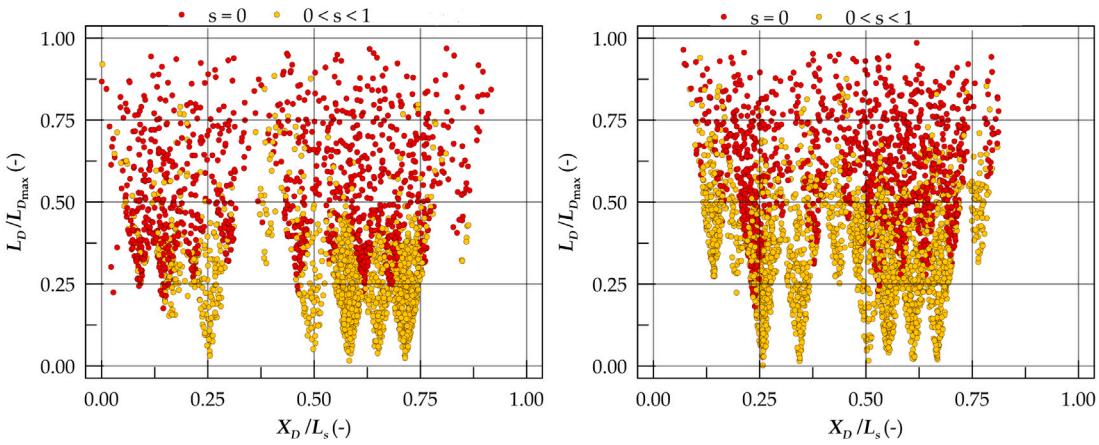

Fig. 9. Damages above 10^{-4} static risk threshold for Ship-A (*left*) and Ship-B (*right*).

Adopting such filtering allows for evaluating vessel survivability with dynamic simulations, evaluating the index A directly from the filtered dataset, considering that the vessel survives the other damages. Therefore, supposing that N_s is the total number of samples and N_F is the number of cases remaining after the filter application, the survivability index becomes:

$$A = 1 - \frac{1}{N_s}\left(N_F - \sum_{i=1}^{N_F} s_i|_{t_{max}}\right) \tag{7}$$

where s_i is the survivability factor of the dynamic simulation evaluated according to Eq. (6). When the assessment refers to calm water, there is no need for repetitions, and the s-factor assumes the value of function I described in Eq. (6), meaning 0 if the vessel capsizes or 1 if survives after t_{max}.

The process described here uses a static s-factor valid for calm water cases as prescribed by SOLAS. However, the methodology applies also to irregular waves adopting an alternative definition of the s-factor in the preliminary calculations [62].

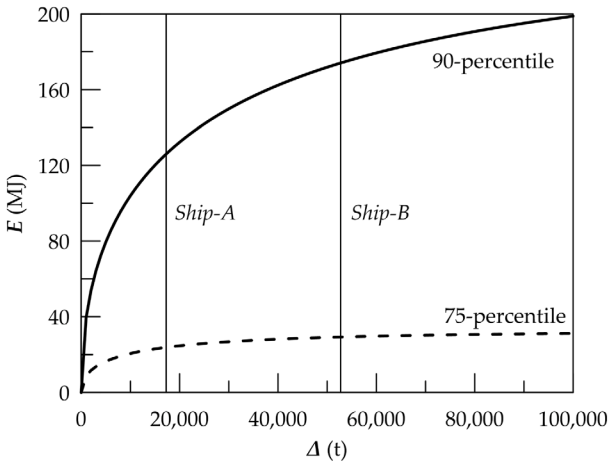

Fig. 10. 75 and 90-percentile energy limits for *Ship-A* and *Ship-B*.

5. Energy method

Another approach could be pursued to filter out minor damages resulting from the non-zonal sampling process of the probabilistic damage stability framework; this time, without the need to perform preliminary static analysis. This approach is based on the energy absorbed by the vessel after an accident. Therefore, it is necessary to adopt a method to evaluate the energy absorbed by the ship after damage with specific geometric characteristics occurring. To this end, several methods could be applied to have a different level of approximations and, consequently, different calculation and pre-processing times. These methods include simple empirical formulae [67,68], analytical methods based on the super-element solutions [69] and finite element modelling techniques [70,71].

Simple empirical formulations require the knowledge of the damage extents and an estimate of the structural volume of the ship related to the damaged area. Super-element method and finite element modelling require knowledge of the vessel's structural components. Finite element methods are certainly more accurate than all the other methods; however, this requires a higher calculation time which is not reasonable to apply especially when considering thousands of damage scenarios.

Regardless of the method used to evaluate impact energy, this energy-based approach requires defining a threshold level that identifies the limit of what can be considered critical damage to the ship. To this end, statistical analyses of collisions are available in the literature [55]. These studies analyse damages deriving from ship to ship accidents, evaluating the associated energy for each impact. Representative curves show an exponential behaviour of the energy absorbed by the struck ship as a function of the ship's displacement. Regression curves identify the 25, 50, 75 and 90-percentile of the energy absorbed by vessel collisions worldwide. These values refer to damages located in the middle of the struck vessel, but they are used here for the whole ship purely as a demonstrative example. Fig. 10 shows the 75 and 90-percentile curves, identifying the respective limits for *Ship-A* and *Ship-B*.

For this explorative application on *Ship-A* and *Ship-B*, the energy associated with every single damage has been calculated through the approximate empirical formulation given by Minorsky [72], as reported in Appendix C. The authors are fully conscious of the simplified nature of the formulation. However, the method calculates an estimated level of energy that is compatible with the early-design stage requirements without knowing the detailed structural layout of the ship under analysis, which is essential to apply more complicated and accurate methods. However, this approach may provide an effective filter for early design stage calculations of damage stability at a sufficient level of granularity.

Fig. 11 presents an overview of the results obtained from this simplified energy method for the two reference ships. Using the 75 and 90-percentile of energy collision distribution as threshold values, 46.7% of the damages for *Ship-B* are above the 75-percentile, whilst 4.9% exceeds the 90-percentile limit. For *Ship-A*, 32.9% of the damage cases are above the 75-percentile, and only 2.0% exceed the 90-percentile of absorbed energy. The different distribution of damages between the two ships influences the obtained results, as *Ship-A* has a higher damage density in the region where low energy is detected, resulting in a higher filtering ratio than *Ship-B*.

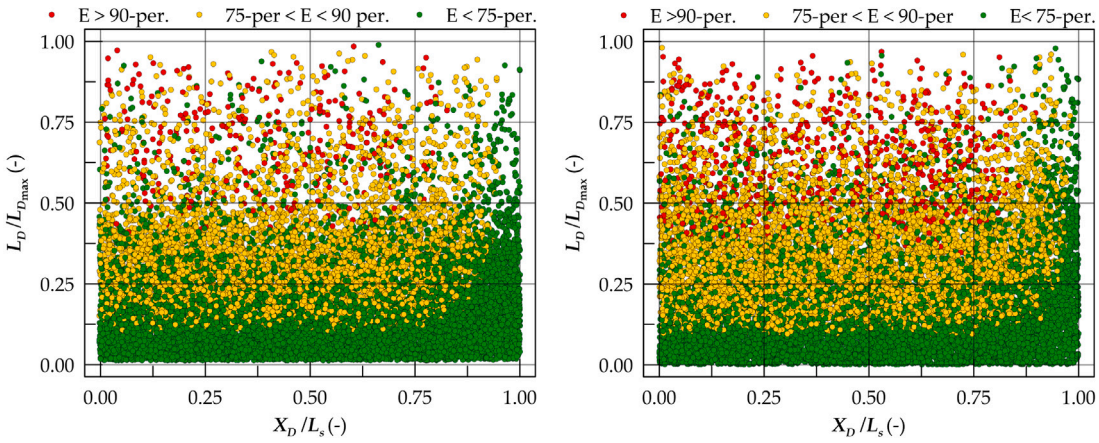

Fig. 11. Energy based damage screening for Ship-A (*left*) and Ship-B (*right*).

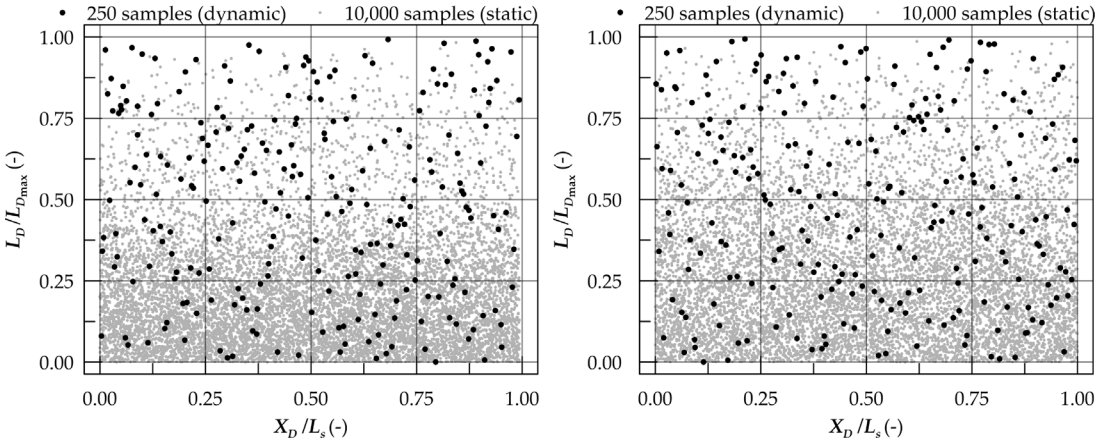

Fig. 12. Comparison between 10,000 SOLAS and 250 uniform damages for Ship-A (*left*) and Ship-B (*right*).

On the other hand, the obtained results reflect the approximate nature of the Minorsky formulation, giving intrinsically more weight to damages with higher penetration. This formula filters out breaches with higher longitudinal and vertical extents but low penetration as they have low absorbed energy. However, these damages result as capsizes in static analysis ($s = 0$) and most likely may be detected as transient capsizes with dynamic simulations.

This filtering process can be applied to the damage samples for dynamic simulations as the final determination of dynamic survivability can be performed according to Eq. (7). Moreover, the energy filter is applicable also in case wave height distribution is sampled for irregular waves calculations.

6. Dynamic screening

The above-described methodologies for damage filtering presuppose that damage cases are sampled from conventionally adopted probabilistic frameworks, thus aiming to determine survivability with either a zonal or non-zonal approach. These approaches are intrinsically derived from static analysis or suppose the availability of a preliminary static assessment. However, an alternative and new vision of the problem can substitute the preliminary static analysis with a reduced set of dynamic simulations.

As mentioned in Section 2, the definition of a damage scenario for a hybrid dynamic analysis considers every single breach generated for static analyses. The same damage set is valid also in the case of a fully dynamic approach adding the wave height as an additional random variable. Therefore, the damage probability distributions recommended by the in-force probabilistic framework for damaged ships can also apply to perform a survivability assessment with a dynamic approach. However, sampling according to the above-mentioned marginal distribution will lead to the same samples shown in Fig. 6 for the two reference ships. These damage distributions have a majority of relatively small damages that do not lead to capsizing in dynamic simulations. However, a Monte Carlo process for survivability determination necessitates the analysis of all these 'safe' cases to obtain the final survivability index value. Instead of directly calculating all the damage cases derived from samples of 10,000 scenarios, it could be interesting to perform an initial set of simulations on a reduced number of scenarios to identify critical areas directly with a dynamic approach. To this end, the marginal distributions provided by SOLAS have to be abandoned, as they intrinsically lead to highly populated relatively small damages. Therefore, the proposed new methodology adopts an initial sample assuming that damage location and dimensions follow uniform distributions.

The newly proposed preliminary analysis follows the following steps:

- *Initial uniform sampling*: sample a number $N_u < N_s$ of damages according to uniform distributions.
- *Preliminary dynamic calculations*: execution of preliminary dynamic simulations in calm water on the reduced damage set with a specific t_{max}.
- *Preliminary results analysis*: analysis of the preliminary dynamic calculations to identify true capsizes or damage cases failing imposed criteria.
- *Damage filtering*: identification of potentially critical cases in the original damage set.

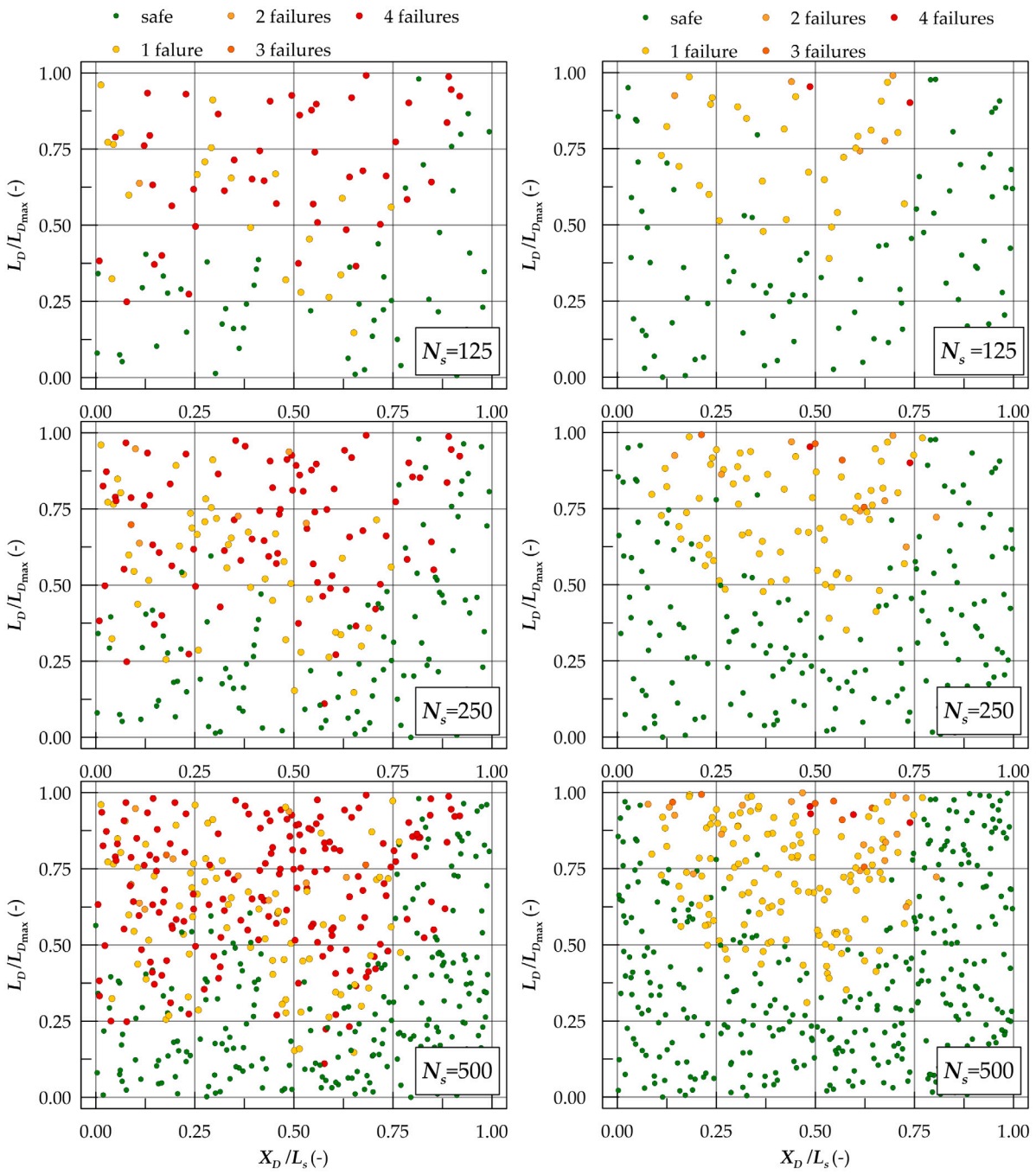

Fig. 13. Preliminary dynamic analysis for Ship-A (*left*) and Ship-B (*right*) considering different sample sizes.

The above-described process is preferably applicable for calm water, thus performing the initial study discarding the presence of waves. The initial calculations can also consider a given significant wave height, showing the influence of irregular waves in a reference sea state on the initial sample. However, the simulation of irregular waves increases the computation time and introduces additional randomness to the process.

The damage generation from uniform distributions relates to three sample sizes (N_s =125, 250, 500) employing the same RQMC sampling technique used for the previous methods. Fig. 12 gives an overview of the new sample for N_s = 250, comparing the points with one of the three N_s = 10,000 samples for static analyses. The figure shows the distribution of non-dimensional damage length L_D against the non-dimensional damage location X_D. It is noteworthy that the uniform sampling populates the region of longer damages with more cases than the standard sampling, thus giving a global coverage of the whole damage space with a significantly lower number of points. The same properties are valid also for the other damage dimensions not reported here for brevity.

By performing dynamic simulations on this set of damages, it is possible to identify the critical cases of this reduced group of scenarios. Besides true capsizes (simulations where the vessel heeling exceeds 90 degrees or where the ship sinks within t_{max}), alternative criteria allow for detecting critical damage scenarios. This study considers the following measures to qualify the outcomes of the simulations:

- *SOLAS heeling failure*: maximum heel above 15 degrees.
- *ITTC maximum heeling*: maximum heeling above 30 degrees.
- *ITTC average roll*: cases where 3 minutes' average roll exceeds 20 degrees.

Table 2
Dynamic failure criteria for *Ship-A* with different sample sizes.

Criterion	N_s		
	125	250	500
True capsize	46	81	167
SOLAS heeling	68	133	259
ITTC heeling	47	86	178
ITTC average roll	46	83	172
Floodwater mass rate	45	80	166
Total	36	133	259

Table 3
Dynamic failure criteria for *Ship-B* with different sample sizes.

Criterion	N_s		
	125	250	500
True capsize	2	2	4
SOLAS heeling	36	84	156
ITTC heeling	2	7	16
ITTC average roll	6	12	21
Floodwater mass rate	2	2	4
Total	36	84	156

- *Final average floodwater mass rate*: simulations where the process is ongoing after t_{max}.

These failure criteria are those usually applied to dynamic simulations in the traditional approach. Fig. 13 shows the output of the preliminary study on the two reference ships, reporting the failure type detected during the 30 min simulations. Results relate to the three sample sizes used as a representative example. The graphical representation identifies the area containing possible critical damages. It is evident that L_D and X_D have a strong influence on the distribution of failure cases. Results show no direct correlation with other damage dimensions, where the criticalities spread through the whole domain and are, therefore, not reported in graphic form.

A more detailed analysis of the results allows for distinguishing between the different failure modes observed for the two reference ships. Table 2 reports the case of *Ship-A*. The uniform distributions permit the detection of a significant number of damages leading to a true capsize, mostly occurring within the transient phase. Besides, Table 3 is representative of *Ship-B*. The large cruise ship case shows fewer failures than *Ship-A*, and only two true capsizes have been spotted. Notably, such a few samples detect two true capsizes, as, applying the same GM, no cases with that nature have been found with the conventional sampling process on 1,000 damages, considering 4 metres of significant wave height H_s. It is worth noticing that using uniform distributions, an increase in sample size proportionally increases the number of critical cases. However, observing Fig. 13, it is possible to recognise the area containing a high failure density without using a large sample size. For both the reported cases, $N_s = 250$ is a valid option to identify the critical region of damages.

This preliminary analysis allows for the formulation of possible filtering strategies. A first rough option is the introduction of an L_D threshold, leading to the generation of a secondary set of samples from the original damage set generated by conventional marginal distributions for damage dimensions and locations. This approach would allow the survivability assessment with a Monte Carlo process (applying equation (7)), considering all damages beyond the L_D threshold as intrinsically safe.

However, the call for methods dealing with first principle tools and physics-based solutions within the FLARE project suggests implementing a more refined filtering methodology. This study investigates the possibility to identify a limiting envelope in the $L_D - X_D$ plain, dividing the failure cases and the safe ones from the preliminary dynamic simulations results. The developed procedure aims at finding a curve that maximises the subtended area while being a lower limit of the detected critical cases. This process is an optimisation problem that maximises the following objective function:

$$\max(z) = \int_{x_{1_{min}}}^{x_{1_{max}}} f\left(x_1, \mathbf{X}\right) \mathrm{d}x_1 \tag{8}$$

where x_1 is the non-dimensional X_D defined in the C00 damage description, $x_{1_{max}}$ and $x_{1_{max}}$ are the maximum and minimum non-dimensional values of the failure cases detected in the preliminary calculations, and $\mathbf{X} = (X_0, \ldots, X_n)$ is the array of the limiting function coefficients corresponding to the n optimisation variables. The problem should include a set of constraints $c(\mathbf{x})$ necessary to ensure that all the N_f points associated in the preliminary dynamic analysis with a failure stay above the limiting curve. Such inequality constraints have the following form:

$$c\left(\mathbf{X}\right) = \begin{cases} f\left(x_{1_1}, \mathbf{X}\right) & < x_{2_1} \\ f\left(x_{1_2}, \mathbf{X}\right) & < x_{2_2} \\ & \vdots \\ f\left(x_{1_{N_f}}, \mathbf{X}\right) & < x_{2_{N_f}} \end{cases} \tag{9}$$

where x_2 is the non dimensional L_D defined in the C00 damage definition. By selecting a continuous polynomial function of grade n as reference $f(\mathbf{x})$, the integral in the objective function assumes the following form:

$$\int_{x_{1_{min}}}^{x_{1_{max}}} f\left(x_1, \mathbf{X}\right) \mathrm{d}x_1 = \sum_{i=0}^{n} X_i \frac{1}{n+1} \left(x_{1_{max}}^{i+1} - x_{1_{min}}^{i+1}\right) \tag{10}$$

equation (10) is then linear in $\mathbf{X}$, and the same applies to the constraints $c(\mathbf{X})$ as they become:

$$c\left(\mathbf{X}\right) = \begin{cases} \sum_{i=0}^{n} X_i x_{1_1}^i & < x_{2_1} \\ \sum_{i=0}^{n} X_i x_{1_2}^i & < x_{2_2} \\ & \vdots \\ \sum_{i=0}^{n} X_i x_{1_{N_f}}^i & < x_{2_{N_f}} \end{cases} \tag{11}$$

For the objective function like equation (10) and constraints like in Eq. (11), it is possible to apply a linear optimisation technique to solve the problem. Here, the presence of inequality constraints makes the problem dual and, therefore, a dual-simplex method has been used to find the optimal limiting curve.

The general problem has no limitations to the polynomial function order used while searching for the optimal solution. For the two tested ships, the implemented procedure allows for using n incrementally up to 8, automatically saving the case with the higher objective function value. The optimisation process has been applied to the two reference ships, considering the initial uniform sampling with $N_s = 250$.

Fig. 14 shows the limiting curve obtained for *Ship-A*, and in such case, the output corresponds to a polynomial function of order $n = 8$. The resulting curve captures all the critical damage cases detected by the initial set of 250 damages. The curve highlights two more critical areas around X_D/L_s 0.2 and 0.6, as it was for the static "risk" profile of Fig. 7. Besides the limit, Fig. 14 also provides the damages of one of the three initial 10,000 breaches samples with the associated static s-factor that actually lay above the limiting curve. The dynamic-based filtering does not discard all the statically safe damages, as those laying above the critical limit. However, compared to the crude static filtering $s \neq 0$, the region of filtered cases is less extended, excluding damages with relative low length. Fig. 15 shows the same outputs for *Ship-B*. The large cruise ship limiting curve is, also in this case, a polynomial function of order $n = 8$. As already highlighted by the preliminary calculations, the area with failure conditions is limited compared to *Ship-A*. Contrarily to the static "risk" profile of Fig. 7, the dynamic failure area develop along

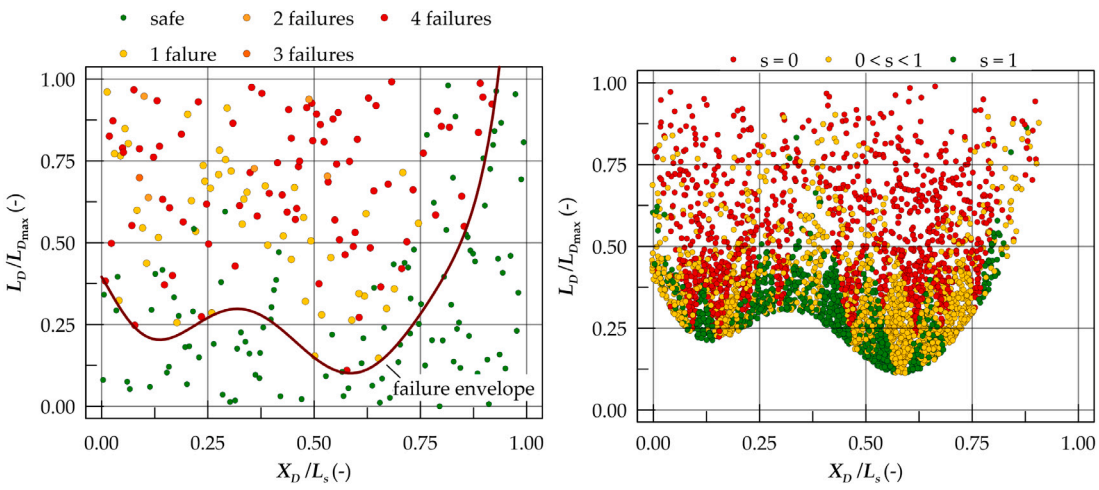

Fig. 14. Filtered breaches for Ship-A (*right*) considering a limiting function from preliminary dynamic simulations (*left*).

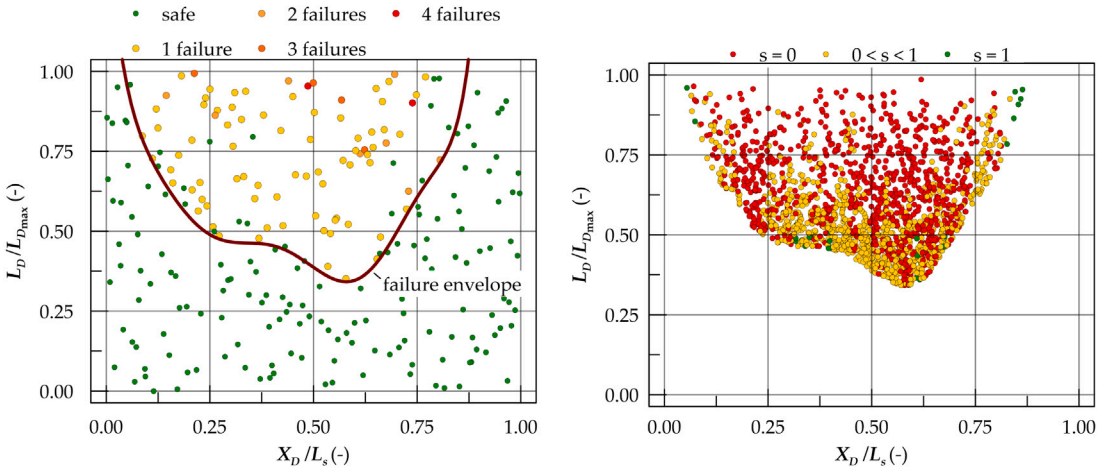

Fig. 15. Filtered breaches for Ship-B (*right*) considering a limiting function from preliminary dynamic simulations (*left*).

amidships with a concentration around X_D 0.6. Looking at the filtered damages from the initial 10,000 breaches, there are few statically safe cases in the critical damages set. Such a matter leads to a consistent reduction of dynamic scenarios compared to static filtering.

The execution of 250 preliminary dynamic simulations does not require significant computational effort. The time domain simulations in calm water run almost three time faster than real time on a regular computer. Moreover, compared to adoption of static calculation, this method used the same criteria conventionally used to assess dynamic simulations.

7. Methods comparison

The three methods described above define different approaches to damage screening during the damage survivability assessment of a passenger ship. That means considering the dynamic analysis as a consequential and complementary process to static analysis (hybrid approach) or considering the dynamic analysis independent from static calculations. All the procedures showed the capability of reducing the number of damage scenarios compared to a traditional complete sampling of damage cases. It is noteworthy that all methods present some positive and negative aspects concerning the number of discarded damages, the modelling simplification and the calculation time.

The filtering based on preliminary static analysis is probably the most straightforward method, directly reflecting the consequentiality of static and dynamic calculations in a damage stability framework. This approach has different options to filter out damage cases. Considering only damages with $s = 0$, solutions with $s \neq 0$, or mitigating the results through the risk threshold in certain areas. On the other hand, for the last option being the most suitable to identify cases for dynamic analysis, the process identifies 2,376 and 2,107 potentially critical damages starting from a 10,000 damages sample for *Ship-A* and *Ship-B*, respectively. The results refer to a "risk" threshold of 1E-4 and report the mean value on the three reference samples of 10,000 damages. Table 4 gives an overview of the filtered cases on all three damage sets. The process has a good performance, discarding about 80% of initial breaches. However, static calculations usually refer to a different internal layout than a dynamic calculation. The ship is modelled only up to the bulkhead deck with simplified compartmentation and fewer relevant openings. This difference could identify more critical cases than what could result from dynamic simulations. Therefore, this method is valid only using the dynamic layout for statics, as performed here for the reference ships.

The energy-based filtering is a different strategy that does not require the execution of preliminary static analysis. In the present work, the method employs a simplified formulation for the absorbed energy determination, and the results reflect the nature of the simplified formulations used. Nevertheless, the process identifies an average of 3,358 and 4,651 critical cases for *Ship-A* and *Ship-B*, respectively, considering the threshold of the 75-percentile of potentially absorbed energy. Thus, the performance is lower than the previous method, but it could significantly improve using the 90-percentile of absorbed energy

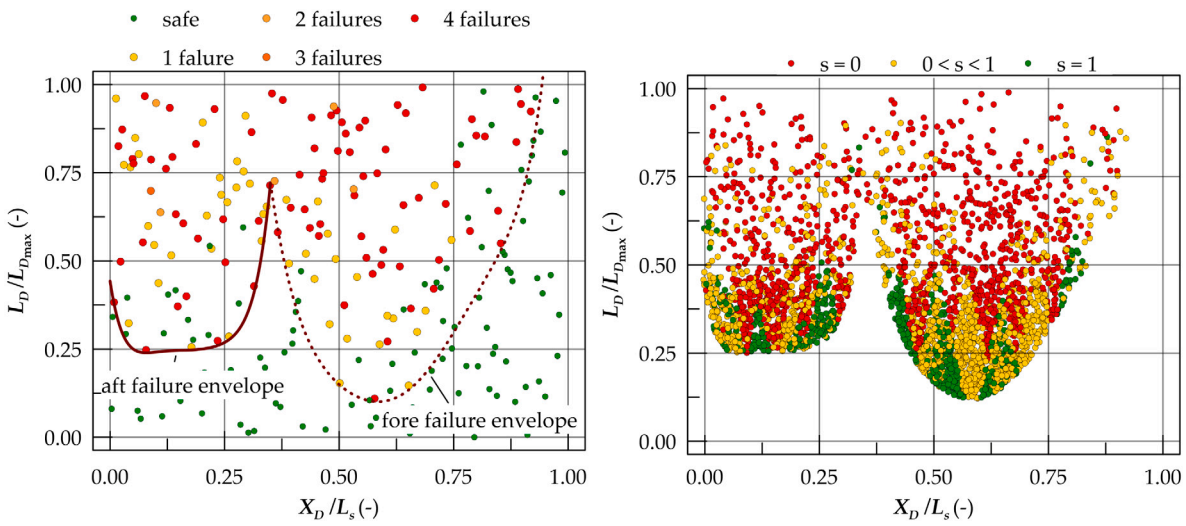

Fig. 16. Filtered breaches for Ship-A (*right*) considering two limiting functions from preliminary dynamic simulations (*left*).

Table 4
Filtered cases for the three initial damage samples for *Ship-A* and *Ship-B*.

Method	Ship-A			Ship-B		
	samp. 1	*samp. 2*	*samp. 3*	*samp. 1*	*samp. 2*	*samp. 3*
Static ($s = 0$)	1102	1127	1129	832	801	841
Static ($s \neq 0$)	3357	3335	3313	3517	3461	3442
Static ($p(1-s) > 10^{-4}$)	2378	2.379	2371	2151	2100	2071
Energy (75 per.)	3387	3389	3297	4688	4625	4641
Energy (90 per.)	203	200	206	488	475	507
Dynamic	3361	3436	3395	1230	1223	1219

(details in Table 4). In conclusion, regardless of the adopted model simplifications, this method strictly depends on the threshold level adopted to filter the damages. Only dedicated studies with high fidelity crash simulation tools can estimate the energy threshold. Moreover, a SOLAS damage distribution is already a potential energy distribution along with the ship. Therefore, this method could be inappropriate for the in-force probabilistic framework but presents an alternative way to generate damages to be further analysed in dedicated studies.

The fully dynamic approach is a different option to face the damage filtering process. The method skips static calculations; thus, there are no additional uncertainties by comparing results from two potentially different internal layouts and opening definitions. Preliminary damage set sampled from a uniform distribution for all the damage characteristics allows for the investigation of the whole damage space with a reduced number of sampling. In this explorative study, after a sensitivity analysis, 250 samples were sufficient to describe the critical areas of the two sample ships; however, the optimal number of cases determination requires further studies on a large ship set. The method identifies the criticality by adopting the same criteria used for traditional dynamic calculations, thus in correspondence with the critical cases of the final runs for survivability assessment. The process identifies 3,397 and 1,224 filtered damages for *Ship-A* and *Ship-B*, respectively (see Table 4). For the large cruise ship, the filtering capability of this method is high, performing better than the static filtering with a "risk" threshold. However, the amount of damages for *Ship-A* is higher compared to the static "risk" filtering. The reason is that the shape of the limiting curve does not exclude a significant portion of space between the two minima. This matter suggests that a more complex limiting function can be studied to improve the filtering capabilities of the process.

As an example, Fig. 16 shows the application of the same process on *Ship-A* using two limiting curves, one for the aft ship and one for the forepart. Such process reduces the filtered cases to about 2,970, more in line with the static risk filtering. However, the number of unfiltered damages is related to the SOLAS length distribution. Smaller ships such as *Ship-A* have an imbalance between damage density of relative long breaches and short ones. Thus, when the limiting curve includes zones with a high density of points, many cases pass the screening. Such a phenomenon is not present for large ships, where the transition between high density and low density of damage length points is smooth (see Fig. 4).

As a final resume, the described filtering strategies may apply to the multi-level damage stability framework for damage stability assessment of passenger ships depicted in Fig. 1. The analysis of the three methods lead to the following conclusions:

- *Static filtering*: the method offers different filtering thresholds, considering the s-factor alone or in combination with the associated p-factor for static analysis. The process requires the execution of a Level 1 static analysis; therefore, it is the most appropriate filtering strategy for the hybrid prediction methodology. The adoption of the static risk profile allows for high filtering performances. However, the method may suffer from the differences in geometrical models employed in static and dynamic simulations.
- *Energy filtering*: the method is actually in an embryonic form. The adopted methodology uses simplified models and tools and needs dedicated research for further development, especially for threshold identification. Nonetheless, the process offers an alternative approach to damage analyses independent of static calculations. Therefore, energy filtering potentially applies to hybrid and fully dynamic Level 2 predictions.
- *Dynamic filtering*: this method is specific for fully-dynamic Level 2 predictions, but there are no contraindications to applying it in the hybrid process. Such a filtering strategy requires a new original procedure for damage definition and preliminary calculations. However, the filtering is independent of static analysis; therefore, if a Level 1 prediction is not required, the initial study substitutes a Level 1 assessment. The main advantage of this novel process is the adoption of the same geometry and criteria within preliminary and final calculations and the possibility of analysing irregular waves conditions.

The described damage screening methodologies have advantages and disadvantages summarised in Table 5. Of the three, static risk filtering is the most applicable method for end-users familiar with static analysis only who want to approach a Level 2 analysis. Dynamic filtering is the proper method to pursue a direct assessment of Level 2 ship survivability, as the filtering process is independent of original damage

Table 5
Advantages and disadvantages of the proposed filtering strategies.

	Static filtering	Energy filtering	Dynamic filtering
Filtering capabilities	High	Average-High	High
Advantages	Easy to understand Easy to apply for a hybrid approach	Independent of static and dynamic analysis Applicable for all the framework options	Same internal layout of Level 2 analysis Same criteria of Level 2 analysis Independent of static analysis Appropriate for a fully dynamic method Easy to apply with custom damage distributions
Disadvantages	Different geometry between Level 1 and Level 2 Different criteria between Level 1 and Level 2	Preliminary structural analysis Definition of threshold	Calculation time

sampling and is coherent with Level 2 analysis of dynamic simulations results. Furthermore, the filtering method may allow to perform more easily calculations aimed at building a database of dynamic simulations suitable to be used for on-board risk assessment tools, instead of relaying on simplified static calculations, as proposed in [5].

8. Conclusions

The present explorative work proposes three different methods to identify critical damage conditions for passenger ships, applying them to two reference passenger ships. The methods have positive and negative aspects, providing solutions that fit into a multi-level damage stability framework but follow radically different paths. The most conventional methods based on static analysis are the direct sum between Level 1 and Level 2 analysis, even though the two levels refer to different geometries and assumptions. In any case, these methods grant a significant reduction of damage cases to analyse with dynamics. Methods from energy-based filtering are still in an embryonic form and need further development and analyses employing more accurate models and tools. However, they could be attractive to figure out possible innovative ways for damage breach generation.

The full dynamic-simulation based approach is the most attractive solution to filter damages, as it represents an application of first-principles tools throughout the damage stability process. The method can also investigate irregular waves in the preliminary phase. However, the calculation time can be higher than the static analysis filtering. The filtering method can be further improved by studying alternative forms for the limiting functions and the identification of the minimum number of initial calculations. Furthermore, the process can be applied to damage types as bottom and side groundings not covered in this study. However, also in the present status, the newly developed dynamic filtering strategy represents a reliable starting point for applying a total direct assessment of damage stability for passenger ships. The process allows for even more extensive and appropriate use of dynamic simulations in a damage stability assessment process for passenger ships.

Further studies need to follow mainly concerning the Energy and the Dynamic methods. The employment of direct calculations for damage generation, not applied here but already employed during the research activities in FLARE, could directly provide the Energy absorbed by the collision. Then, attention should be given in finding a correlation between the energy level absorbed in the impact and the survivability of the ship after the impact. Such a study will avoid the use of empirical correlation to establish the critical filtering thresholds.

On the other hand, the dynamic filtering has shown good performances for collision, clearly identifying the main damage dimensions influencing most ship survivability. The considerations are limited to collisions and should be carefully checked also for the other damage types considered in the multi-level damage stability framework, i.e. bottom and side groundings. It could be the case that other damage parameters are relevant for ship survivability besides position and length, especially for bottom groundings where the damage could extend also starting from different transversal position under the hull and leading to different functions to be studied to limit the critical domain for survivability.

CRediT authorship contribution statement

Francesco Mauro: Writing – review & editing, Writing – original draft, Visualization, Validation, Software, Methodology, Investigation, Formal analysis, Data curation, Conceptualization. **Dracos Vassalos:** Writing – review & editing, Supervision, Funding acquisition. **Donald Paterson:** Writing – review & editing, Validation.

Declaration of competing interest

The authors declare that they have no known competing financial interests or personal relationships that could have appeared to influence the work reported in this paper.

Data availability

Data will be made available on request.

Acknowledgements

The financial support of the EU project FLARE is acknowledged. The information and views set out in this paper are those of the authors and do not necessarily reflect the official opinion of all FLARE partners.

Appendix A. Randomised Quasi-Monte Carlo sampling

The non-zonal approach method to generate damages allows the application of non-deterministic Monte Carlo (MC) integration to evaluate the Attained survivability index. Eqs. (3) and (5) are already representative of a multidimensional MC integration process. In such a case, the integral value I_{MC} has the following form:

$$I_{MC} = \int_{\Omega} f(\mathbf{x})\,\mathrm{d}\mathbf{x} \approx \frac{1}{N_s}\int_{\Omega} \mathrm{d}\mathbf{x} \sum_{i=1}^{N_s} f(\mathbf{x}_i) \tag{12}$$

where $\Omega \subset \mathbb{R}^m$ is a m-dimensional probability space, $\mathbf{x} = (x_1, \ldots, x_m) \in \Omega$ is a set of independent random variables and N_s is the number of samples. Considering the probability space as a unit hypercube $\Omega = (0,1)^m$, the integral on Ω becomes 1 and I_{MC} is determined by the summation part only. It is also possible describe $\mathbf{x}$ by uniform random variables $\mathbf{U} = (u_1, \ldots, u_m) \in (0,1)^m$; then, direct sampling of $\mathbf{U}$ through pseudo-random numbers represents the standard crude MC method [73]. According to the strong law of large numbers, the approximated integral always converges to the exact value as N_s increases without bounds. Besides, the process is subject to uncertainties that

asymptotically reduce increasing N_s. A possible way to decrease the uncertainties without increasing N_s is replace the independent random variables $\mathbf{U}$ by a set of deterministic points $\mathbf{P}_m = (p_1, \ldots, p_m)$ that cover the space Ω more evenly. Such deterministic points are usually referred as low discrepancy sequences and grants a faster convergence than crude MC in the evaluation of an integral. Here use has been made of Sobol low discrepancy sequence [74,75], where the generation starts from the selection of a set of polynomials of n_j degree $P_j = x^{n_j} + a_{1,j}x^{n_j-1} + a_{2,j}x^{n_j-2} + \cdots + a_{n_j-1,j}x + 1$, where coefficients $a_{i,j}$ are either 0 or 1, are used to generate a sequence of positive integer numbers according to the following recursive relation:

$$m_{k,j} = 2a_{1,j}m_{k-1,j} \oplus 2^2 a_{2,j}m_{k-2,j} \oplus \cdots \oplus 2^{n_j} m_{k-n_j,j} \oplus m_{k-n_j,j} \tag{13}$$

where $\oplus$ is the bit-by-bit exclusive-or operator, $1 \le k \le n_j$ is odd and $n_j \le 2^k$. Finally, the jth component of the ith point of the Sobol sequence is given by:

$$x_{i,j} = i_1 v_{1,j} \oplus i_2 v_{2,j} \oplus \cdots \tag{14}$$

where $v_{i,j} = m_{i,j}/2^k$ and i_k is the kth binary digit of i. The process can be implemented in software programs, generating Sobol sequences with low computational effort [76,77].

However the adoption of a low discrepancy sequence, usually referred as deterministic Quasi-Monte Carlo (QMC) method, does not allow for a straightforward evaluation of the integration error. A Randomised Quasi-Monte Carlo (RQMC) method allows to re-randomise the low discrepancy sequence, transforming sequence points p_i in random points x_i that retain QMC properties method and expectation of I_{MC}. The randomisation process is performed by applying a left linear matrix scramble [78,79] followed by a random digital shift to ensure a uniform distribution of the scrambled points.

In the case of damage sampling, the evaluation of the integral requires damage stability calculations on a set of breaches, whose characteristics derives from the inversion process of cumulative density functions given in Appendix B. The sampling is based upon the following general property; if F is a continuous cumulative density function in $\mathbb{R}$ with inverse F^{-1} defined by:

$$F^{-1}(u) = \inf\{x : F(x) = u, 0 \le u \le 1\} \tag{15}$$

then, if $\mathbf{U}$ is a uniform random variable in $[0,1]$, the inverse $F^{-1}(\mathbf{U})$ is distributed according to F. This is true also for distribution with finite support, as in the case of damage breach characteristics. In general, the procedure for a generic array of random variables $\mathbf{x}$ with RQMC method can be summarised in the following steps, assuming we know the starting $f(\mathbf{x})$ for the final sample:

1. Compute the cumulative density function $F(\mathbf{x})$.
2. Compute the inverse $F^{-1}(\mathbf{x})$.
3. Generate the QMC low discrepancy datasets $\mathbf{P}_m$ $(0,1)$ with a Sobol sequence using code given by [77].
4. Generate the RQMC sets $\mathbf{U}_m$ $(0,1)$ with linear matrix scramble and random digital swift as indicated by [79].
5. Compute $F^{-1}(\mathbf{U})$.

The described procedure can be easily applied to the distributions described in Appendix B for C00 collisions or for any kind of damage types.

Appendix B. C00 collision damage probabilistic model

The sampling process for C00 damages requires the inversion of cumulative distributions describing the potential damage characteristics introduced in Section 2.1. The marginal distributions are derived in such a way to be compliant with SOLAS2009 [25] indications, with the addition of the lower limit of vertical extent. The probabilistic model is reported here using the non-dimensional notation in compliance with the distributions shown in Figs. 2 and 3. Therefore, all the presented random variables are defined in $[0,1]$.

The longitudinal position of the damage centre X_D is assumed to be uniformly distributed along the ship subdivision length L_s. Therefore, the associated non-dimensional variable $x_1 = \frac{X_D}{L_s}$ has the following cumulative and density function, respectively:

$$F(x_1) = x_1 \tag{16}$$

$$f(x_1) = 1 \tag{17}$$

The probabilistic modelling tor the damage length L_D depends on the ship length L_s, as the maximum damage length $L_{D_{max}}$ necessary to define $x_2 = \frac{L_D}{L_{D_{max}}}$ is determined as follows:

$$L_{D_{max}} = J_m L_s \text{ where } J_m = \begin{cases} \frac{10}{33} & \text{if } L_s \le 198 \text{ m} \\ \frac{60}{L_s} & \text{if } L_s > 198 \text{ m} \end{cases} \tag{18}$$

Then the marginal cumulative and density functions for x_2 are as follows:

$$F(x_2) = \begin{cases} 0.5b_{11}J_m^2 x_2^2 + b_{12}J_m x_2 & \text{if } x_2 \le J_k \\ 0.5b_{11}J_m^2 J_k^2 + b_{12}J_m J_k & \\ \quad +0.5b_{21}J_m^2\left(x_2^2 - J_k^2\right) + b_{22}J_m\left(x_2 - J_k\right) & \text{if } x_2 > J_k \end{cases} \tag{19}$$

$$f(x_2) = \begin{cases} b_{11}J_m^2 x_2 + b_{12}J_m & \text{if } x_2 \le J_k \\ b_{21}J_m^2 x_2 + b_{22}J_m & \text{if } x_2 > J_k \end{cases} \tag{20}$$

where the parameters appearing in the distributions can be calculated according to the following expressions:

$$J_k = \begin{cases} \frac{J_m}{2} & \text{if } L_s \le 198 \text{ m} \\ \frac{J_m}{2} + \frac{1}{11}\left(1 - \sqrt{\frac{121J_m^2}{4} - \frac{55}{6}J_m + 1}\right) & \text{if } 198 < L_s \le 260 \text{ m} \\ \frac{59}{66}J_m - \frac{\sqrt{335}}{66}J_m & \text{if } L_s > 260 \text{ m} \end{cases} \tag{21}$$

$$b_{11} = \frac{1}{3J_k\left(J_m - J_k\right)} - \frac{11}{6J_k^2} \tag{22}$$

$$b_{12} = \begin{cases} 11 & \text{if } L_s \le 198 \text{ m} \\ 11 & \text{if } 198 < L_s \le 260 \text{ m} \\ \frac{11}{6J_k} + \frac{1}{6(J_k - J_m)} & \text{if } L_s > 260 \text{ m} \end{cases} \tag{23}$$

$$b_{21} = -\frac{1}{6\left(J_m - J_k\right)^2} \tag{24}$$

$$b_{22} = -b_{21}J_m \tag{25}$$

The marginal cumulative and density distributions for the nondimensional penetration $x_3 = 2\frac{B_D}{B}$ have the following formulations:

$$F(x_3) = \frac{1}{5}\left(-3x_3^2 + 8x_3\right) \tag{26}$$

$$f(x_3) = \frac{1}{5}\left(-6x_3 + 8\right) \tag{27}$$

The lower vertical limit of the damage is described by the independent random variable $x_4 = \frac{z_{LL}}{T}$, having the following marginal cumulative and density functions:

$$F(x_3) = \frac{1}{5}\left(-2x_3^2 + 7x_3\right) \tag{28}$$

$$f(x_3) = \frac{1}{5}\left(-4x_3 + 7\right) \tag{29}$$

The upper vertical limit is measured from the ship draught considered for the analysis and is identified by the independent random variable $x_5 = \frac{z_{UL}}{z_{max}}$, where $z_{max} = 12.5$. The associated marginal cumulative and density distributions have the following form:

$$F(x_5) = \begin{cases} 0.8\frac{x_5}{0.624} & \text{if } x_5 \le 0.624 \\ 0.8 + 0.2\frac{12.5x_5 - 7.8}{4.7} & \text{if } x_5 > 0.624 \end{cases} \tag{30}$$

$$f\left(x_5\right)=\begin{cases}\frac{0.8}{0.624} & \text{if } x_5 \le 0.624\\ 0.2\frac{x_5}{0.376} & \text{if } x_5 > 0.624\end{cases} \tag{31}$$

In addition, it can be considered that the damage occurs with the same probability on each side of the vessel. This results in a probability mass function (PMF) for the random variable I_{side} describing the damage side:

$$PMF\left(I_{side}\right)=\begin{cases}P\left(I_{side}=1\right)=\alpha\\ P\left(I_{side}=-1\right)=1-\alpha\end{cases} \tag{32}$$

where $\alpha = 0.5$. $I_{side} = 1$ and $I_{side} = -1$ indicate starboard and port side, respectively.

Appendix C. Empirical Minorsky method

Collision simulation models evaluate energy associated with a ship to ship collision by the analysis of structure deformation on both the striking and struck ship. However, besides these advanced analysis techniques also empirical formulations have been developed for a fast estimation of the energy absorbed during a collision. From the analysis of 26 collision cases on full-scale ship accidents Minorsky derived the following empirical formulation:

$$E = 47.2R_T + 32.7 \tag{33}$$

where E is determined in MJ and R_T is the volume of destroyed material on the striking and the struck ships. R_T takes into account the principal structural elements of the two vessels involved in the collisions, neglecting the side shell of the struck ship. As the formulation is extremely simple, it is still quite often used in collision analyses to have an initial prevision of the absorbed energy. There are some elaborations of the formula considering additional regression terms as function of the thickness of the structure elements. However, such terms did not provide relevant correlation benefits compared to the damage volume term. Therefore the Minorsky formula indicates that the absorbed energy of a ship is proportional to the destroyed volume of material during the collision event. This is not always true but can be acceptable for a preliminary estimation when striking and struck vessel characteristics are not known.

The application of the Minorsky formula requires in principle the knowledge of the destroyed volume also for the striking ship. As in the present work the characteristics of the striking ship are not known, the estimate of the destroyed volume R_T is referred to the struck ship only. Such an assumption imply considering the sticking ship as infinitely stiff, something that is often applied also in more advanced FEM analyses. Therefore, R_T is here directly associated with the dimensions of the collision damage (length L_D, penetration B_D and height $z_{UL}+(T-z_{LL})$), assuming an average thickness for the struck ship in the damage area.

References

[1] Papanikolaou A. Risk-based ship design: Methods, tools and applications. Springer; 2009.
[2] IMO. International convention for the safety of life at sea (SOLAS). Technical report, IMO, Consolidated edition as of 2020; 2020.
[3] Zang M, Conti F, Le Sourne H, Vassalos D, Kujala P, Lindroth D, Hirdaris S. A method for the direct assessment of ship collision damage and flooding risk in real conditions. Ocean Eng 2021;237:109605.
[4] Montewka J, Manderbacka T, Ruponen P, Tompuri M, Gil M, Hirdaris S. Accident susceptibility index for a passenger ship - A framework and case study. Reliab Eng Syst Saf 2022;218:108145.
[5] Ruponen P, Montewka J, Tompuri M, Manderbacka T, Hirdaris S. A framework for onboard assessment and monitoring of flooding risk due to open watertight doors for passenger ships. Reliab Eng Syst Saf 2022;226:108666.
[6] Montewka J, Goerlandt F, Kujala P. On a systematic perspective on risk for formal safety assessment (FSA). Reliab Eng Syst Saf 2014;127:77–85.
[7] Goerlandt F, Montewka J. Maritime transportation risk analysis: Review and analysis in light of somefundational issue. Reliab Eng Syst Saf 2015;138:115–34.
[8] Puisa R, McNay J, Montewka J. Maritime safety: Prevention versus mitigation? Saf Sci 2021;136:105151.
[9] Gil M, Koziol P, Wrobel K, Montewka J. Know your safety indicator - A determination of merchant vessels bow crossing range based on big data analytics. Reliab Eng Syst Saf 2022;220:108211.
[10] Du L, Goerlandt F, Kujala P. Review and analysis of methods for assessing maritime waterway risk based on non-accident critical events detected from AIS data. Reliab Eng Syst Saf 2020;200:106933.
[11] Szlapczynski R, Slzlapczyska J. A ship domain-based model of collision risk for near-miss detection and collision allert systems. Reliab Eng Syst Saf 2021;214:107766.
[12] Gil M. A concept of critical safety area applicable for an ostacle-avoidance process for manned and autonomous ships. Reliab Eng Syst Saf 2021;214:107806.
[13] Zhang M, Zhang D, Fu S, Kujala P, Hirdaris S. A predictive analytics method for maritime traffic flowcomplexity estimation in inland waterways. Reliab Eng Syst Saf 2022;220:108317.
[14] Montewka J, Ehlers S, Goerlandt F, Hinz T, Tabri K. A framework for risk assessment for maritime transportation systems- A case study for open seas collisions involving RoPax vessels. Reliab Eng Syst Saf 2014;124:142–57.
[15] de Vos J, Hekkenberg RG, Koelman HJ. Damage stability requirements for autonomous ships based on equivalent safety. Saf Sci 2020;130:104865.
[16] Vanem E, Skjong R. Designing for safety in passenger ships utilizing advanced evacuation analyses- A risk based approach. Saf Sci 2006;44:111–35.
[17] Spyrou KJ, Koromila IA. A risk model of passenger ship fire safety and its application. Reliab Eng Syst Saf 2020;200:106937.
[18] Montewka J, Goerland F, Innes-Jones G, Owen D, Hifi Y, Puisa R. Enhancing human performance in ship operations by modifying global design factors at the design stage. Reliab Eng Syst Saf 2017;159:283–300.
[19] Wu B, Yip T, Yan X, Guedes Soares C. Review of techniques and challenges of human and organizational factors analyis in maritime transportation. Reliab Eng Syst Saf 2022;219:108249.
[20] Du L, Banda O, Huang Y, Goerlandt F, Kujala P, Zhang W. An empirical ship domain based on evasive maneuver and perceived collision risk. Reliab Eng Syst Saf 2021;214:107752.
[21] Vassalos D. The role of damaged ship dynamics in addressing the risk of flooding. Ships Offshore Struct 2022;17(2):279–303.
[22] Atzampos G. A holistic approach to damage survivability assessment of large passenger ships (Ph.D. thesis), University of Strathclyde; 2019.
[23] Papanikolaou A, Hamman R, Lee B, Mains C, Olufsen O, Vassalos D, Zaraphonitis G. GOALDS: Goal based damage ship stability and safety standards. Accid Anal Prev 2013;60:353–65.
[24] Vanem E, Rusas S, Skjong R, Olufsen O. Collision damage stability of passenger ships: Holistic and risk-based approach. Int Shipbuild Prog 2007;54(4):323–37.
[25] IMO. SOLAS-international convention for the safety of life at sea. Technical report, London, UK: IMO; 2009.
[26] Bulian G, Cardinale M, Dafermos G, Lindroth D, Ruponen P, Zaraphonitis G. Probabilistic assessment of damaged survivability of passenger ships in case of groundings or contact. Ocean Eng 2020;218:107396.
[27] Ruponen P, Lindroth D, Routi A, Aartovaara M. Simulation-based analysis method for damage survivability of passenger ships. Ship Technol Res 2019;66:180–92.
[28] Spanos D, Papanikolaou A. On the time dependance of survivability of ROPAX ships. J Mar Sci Technol 2012;17:40–6.
[29] Bulian G, Cardinale M, Dafermos G, Eliopoulou E, Francescutto A, Hamann R, Linderoth D, Luhmann H, Ruponen P, Zaraphonitis G. Considering collision, bottom grounding and side grounding/contact in a common non-zonal framework. In: 17th International ship stability workshop. 2019.
[30] Vassalos D, Paterson D. Towards unsinkable ships. Ocean Eng 2021;232:109096.
[31] Karolius K, Cichowicz J, Vassalos D. Risk-based positioning of flooding sensors to reduce prediction uncertainty of damage survivability. In: 13th International conference of ships and ocean vehicles. 2018.
[32] Vassalos D. Damage survivability of cruise ships - evidence and conjecture. Ocean Eng 2016;121:89–97.
[33] Mauro F, Paterson D, Michalec R, Boulougouris E, Vassalos D. A damage sampling method to reduce A-index standard deviation in the probabilistic assessment of ship survivability using a non-zonal approach. In: 1st International conference on the stability and safety of ships and ocean vehicles. Glasgow, Scotland, UK; 2021.
[34] Mauro F, Vassalos D. The influence of damage breach sampling process on the direct assessment of ship survivability. Ocean Eng 2022;250:111008.
[35] Papanikolaou A. Review of damage stability of ships - recent developments and trends. In: 10th International symposium on practical design of ships and other floating structures. PRADS, Houston, USA; 2007.
[36] Bačkalov I, Bulian G, Cichowicz J, Eliopoulou E, Konovessis D, Leguen J, Rosén A, Themelis N. Ship stability, dynamics and safety: Status and perspectives from a review of recent STAB conferences and ISSW events. Ocean Eng 2016;116:312–49.
[37] Manderbacka T, Themelis N, Bačkalov I, Boulougouris E, Eliopoulou E, Hashimoto H, Konovessis D, Leguen J, Miguez-Gonzalez M, Rodriguez C, Rosén A, Ruponen P, Shigunov V, Schreuder M, Terada D. An overview of the current research on stability of ships and ocean vehicles: The STAB 2018 perspective. Ocean Eng 2019;186:1–16.

[38] Ruponen P, Valanto P, Acanfora M, Dankowski H, Lee G, Mauro F, Murphy A, Rosano G, van't Veer R. Results of an international benchmark study on numerical simulation of flooding and motions of a damaged ropax ship. Appl Ocean Res 2022;123:103153.
[39] Dankowski H. A fast and explicit method for the simulation of flooding and sinkage scenarios on ships (Ph.D. thesis), Hamburg University of Technology; 2013.
[40] Braidotti L, Mauro F. A fast algorithm for onboard progressive flooding simulation. J Mar Sci Eng 2020;8(5):369.
[41] Ruponen P. Adaptive time step in simulation of progressive flooding. Ocean Eng 2014;78:35–44.
[42] Jasionowski A. An integrated approach to damage ship survivability assessment (Ph.D. thesis), University of Strathclyde; 2001.
[43] de Kat J. Contemporary ideas on ship stability. Elsevier Science Ltd.; 2000, p. 249–63, chapter Dynamics of a ship with partially flooded compartment.
[44] Letizia L. Damage survivability of passenger ships in a seaway (Ph.D. thesis), University of Strathclyde; 1997.
[45] Papanikolaou A, Zaraphonitis G, Spanos D, Boulougouris E, Eliopoulou E. Investigation into the capsizing of damaged ro-ro passenger ships in waves. In: 7th International conference on stability of ships and ocean vehicles. STAB, Launceston, Tasmania, Australia; 2000.
[46] Acanfora M, Cirillo A. A simulation model for ship response in flooding scenario. Proc Inst Mech Eng Part M J Eng Marit Environ 2017;231.
[47] Manderbacka T, Ruponen P. The impact of the inflow momentum on the transient roll response of a damaged ship. Ocean Eng 2016;120:346–52.
[48] Lee GJ. Dynamic orifice flow modeland compartment modelsfor flooding simulations of a damaged ship. Ocean Eng 2015;109:635–53.
[49] Janßen C, Bengel S, Rung T, Dankowski H. A fast numerical method for internal flood water dynamics to simulate water on deck and flooding scenarios of ships. In: ASME 32nd international conference on ocean, offshore and arctic engineering. Nantes, France; 2013.
[50] Santos T, Guedes Soares C. Study of damaged ship motions taking into account floodwater dynamics. J Mar Sci Technol 2008;13:291–307.
[51] Ruth E, Rognebakke O. CFD in damage stability. In: Proceedings of the 17th international ship stability workshop. Helsinki, Finland; 2019, p. 259–63.
[52] Sadat-Hosseini H, Kim D, Carrica P, Rhee S, Stern F. URANS simulations for a flooded ship in calm water and regular beam waves. Ocean Eng 2016;120:318–30.
[53] Zang M, Montewka J, Manderbacka T, Kujala P, Hirdaris S. A big data analytics method for the evaluation of ship-ship collision risk reflecting hydrometeorological conditions. Reliab Eng Syst Saf 2021;213:107674.
[54] Conti F, Le Sourne H, Vassalos D, Kujala P, Lindroth D, Kim S, Hirdaris S. A comparative method for scaling SOLAS collision damage distributions based on a ship crashworthiness application to probabilistic damage analysis of a passenger ship. Ship Offshore Struct 2022;17(7):1498–514.
[55] Lützen M. Ship collision damage (Ph.D. thesis), Technical University of Denmark; 2001.
[56] Pawlowski M. Subdivision and damaged stability of ships. Euro-MTEC book series, Gdansk, Poland; 2004.
[57] Zaraphonitis G, Bulian G, Lindroth D, Hamann R, Luhmann H, Cardinale M, Routi A, Bertin R, Harper G. Evaluation of risk from ranking damages due to grounding. Technical report, DNV-GL 2015-0168 Rev. 2, Project EMSA/OP/10/2013; 2015.
[58] Bulian G, Lindroth D, Ruponen P, Zaraphonitis G. Probabilistic assessment of damaged ship survivability in case of grounding: Development and testing of a direct non-zonal approach. Ocean Eng 2016;120:331–8.
[59] Zaraphonitis G, Bulian G, Hamann R, Eliopoulou E, Cardinale M, Luhmann H. eSAFE-D2.2.1 - Description of methodology. Technical report, Joint Industry Project eSAFE; 2017.
[60] Bulian G, Francescutto A. Probability of Flooding Due to Grounding Damage Using a P-Factor Formulation. Technical report, GOALDS Project; 2010.
[61] Vassalos D, Mujeeb-Ahmed P, Paterson D, Mauro F, Conti F. Probabilistic damage stability for passenger ships - the p-factor illusion and reality. J Mar Sci Eng 2022;10(3):348.
[62] Cichowicz J, Tsakalakis N, Vassalos D, Jasionowski A. Damage survivability of passenger ships - re-engineering the safety factor. Safety 2016;2(4):1–18.
[63] Paterson D, Atzampos G, Vassalos D, Boulougouris E. Impact of wave statistics on ship survivability. In: 16th International ship stability workshop. Belgrade, Serbia; 2017.
[64] Pierson W, Moskowitz L. A proposed Spectral Form for Fully developed Wind Seas based on the simularity theory of S.A. Kitaigorodski. Technical report, U.S. Naval Oceanographic Office, C-62306-1042; 1963.
[65] Hasselmann K, Olbers D. Measurements of wind-wave growth and swell decay during the joint north sea wave project (JONSWAP). Ergänzung Zur Deut Hydrogr Z Reihe A 1973;8(12):1–95.
[66] IMO. SOLASII-2/Reg.21-Causality threshold, safe return to port and safe areas. Technical report, IMO, London, UK; 2016.
[67] Hong L, Amdahl J. Plastic mechanism analysis of the resistance of ship longitudinal girders in grounding and collisions. Ships Offshore Struct 2008;3(3):159–71.
[68] Pedersen T, Zhang S. Absorbed energy in ship collisions and groundings: Revising Minorsky's empirical method. J Ship Res 1998;44(2):140–54.
[69] Buldgen L, Le Sourne H, Besnard N, Rigo P. Extension of the super-element method to the analysis of the oblique collision between two ships. Mar Struct 2012;29:22–57.
[70] GLykas J, Das K. Energy conservation during grounding with rigid slopes. Ocean Eng 2001;28(4):397–415.
[71] Zhang A, Suzuki K. Dynamic FE simulations of the effect of selected parameters on grounding test results of bottom structures. Ship Offsshore Struct 2006;1(2):117–25.
[72] Minorsky V. An analysis of ship collision with reference to protection of nuclear power ships. J Ship Res 1959;3:208–14.
[73] Hammersley J, Handscomb D. Monte Carlo Methods. Methuen & co LTD; 1964.
[74] Niederreiter H. Low-discrepancies and low-dispersion sequencies. J Number Theory 1988;30:51–70.
[75] Sobol I, Asotky D, Krenin A, Kucherenko S. Construction and comparison of high-dimensional Sobol'generators. Wilmott J 2011;64–79.
[76] Levitan Y, Markovich N, Rozin S, Sobol I. On quasi-random sequences for numerical calculations. USSR Comput Math Math Phys 1988;28(5):755–9.
[77] Bradley P, Fox B. Algorithm 659: Iimplementing Sobol's quasi random sequence generator. ACM Trans Math Software 1988;14(1):88–100.
[78] Matousek J. On the L-2 discrepancy for anchored boxes. J Complexity 1998;14(4):527–56.
[79] Hong HS, Hickernell FJ. Algorithm 823: Implementing scrambled digital sequencies. ACM Trans Math Software 2003;29(2):95–109.